Chapter 3
Nonsmooth Processes as Asymptotic Limits

The objective of this chapter is to show that nonsmooth processes may naturally occur as high-energy asymptotics in different oscillatory models with no intentionally introduced stiff constraints or external impacts. In other words, nonsmooth temporal mode shapes may be as natural as sine waves generated by same oscillators under low-energy conditions. Essentially nonlinear phenomena, such as nonlinear beats and energy localization, are also considered. It is shown that energy exchange between two oscillators may possess hidden nonsmooth behaviors.

3.1 Lyapunov's Oscillator

Let us consider a family of oscillators described by the differential equation

$$\ddot{x} + x^{2n-1} = 0 \tag{3.1}$$

where n is a positive integer; see Fig. 1.1.

In the particular case $n = 1$, one has the harmonic oscillator whose natural frequency is unity. When $n > 1$ the system becomes essentially nonlinear and cannot be linearized within the class of vibrating systems. Moreover, as the parameter n increases, the temporal mode shape of oscillator (3.1), while remaining smooth, is gradually approaching the triangle wave nonsmooth limit. Such transitions usually represent a challenging problem from both physical and mathematical viewpoints. Hence it is important to understand some basic cases, such as oscillator (3.1) and those considered in the next section. These special cases admit exact solutions showing explicitly how smooth motions are approaching their nonsmooth limits. It is known regarding oscillator (3.1) that, for an arbitrary positive integer n, its general

V. N. Pilipchuk, *Oscillators and Oscillatory Signals from Smooth to Discontinuous*,
https://doi.org/10.1007/978-3-031-37788-4_3

solution can be expressed in terms of special Lyapunov functions [76, 101, 126], such as $\mathrm{sn}\theta$ and $\mathrm{cs}\theta$ defined by expressions[1]

$$\theta = \int_0^{\mathrm{sn}\theta} \left(1 - nz^2\right)^{\frac{1-2n}{2n}} dz, \qquad \mathrm{cs}^{2n}\theta + n\,\mathrm{sn}^2\theta = 1$$

These functions possess the properties,

$$\mathrm{cs}0 = 1, \qquad \mathrm{sn}0 = 0, \qquad \frac{d\mathrm{sn}\theta}{d\theta} = \mathrm{cs}^{2n-1}\theta, \qquad \frac{d\mathrm{cs}\theta}{d\theta} = -\mathrm{sn}\theta$$

and their normalized period is given by

$$T = 4\sqrt{n}\int_0^1 \frac{dx}{\sqrt{1-x^{2n}}} = 2\sqrt{\frac{\pi}{n}}\frac{\Gamma\left(\frac{1}{2n}\right)}{\Gamma\left(\frac{n+1}{2n}\right)}$$

The general solution of Eq. (3.1) can be written as

$$x = A\mathrm{cs}\left(A^{n-1}t + \alpha\right) \tag{3.2}$$

where A and α are arbitrary constants.

Note that the scaling factors A and A^{n-1} are easily predictable based on the form of Eq. (3.1) since the equation admits the group of transformations $x = A\bar{x}(\bar{t})$, where $\bar{t} = A^{n-1}t$.

For $n = 1$ the functions $\mathrm{sn}\theta$ and $\mathrm{cs}\theta$ give the standard pair of trigonometric functions $\sin\theta$ and $\cos\theta$, respectively. Interestingly enough, the strongly nonlinear limit $n \to \infty$ also gives a quite simple pair of periodic functions. Despite some mathematical challenges, this case admits interpretation by means of the total energy

$$\frac{\dot{x}^2}{2} + \frac{x^{2n}}{2n} = \frac{1}{2} \tag{3.3}$$

where the number $1/2$ on the right-hand side corresponds to the initial conditions $x(0) = 0$ and $\dot{x}(0) = 1$.

Taking into account that the coordinate of the oscillator reaches its amplitude value at zero kinetic energy gives the estimate $-n^{1/(2n)} \le x(t) \le n^{1/(2n)}$ for any time t. Since $n^{1/(2n)} \longrightarrow 1$ as $n \longrightarrow \infty$ then the limiting motion is restricted by the interval $-1 \le x(t) \le 1$. Inside of this interval, the second term on the left-hand side of expression (3.3) vanishes and hence, $\dot{x} = \pm 1$ or $x = \pm t + \alpha_{\pm}$, where

[1] Another version of special functions for Eq. (3.1) was considered in [209].

$\alpha_{\pm}$ are constants. By manipulating with the signs and constants, one can construct the triangle wave, $\tau(t)$, since there is no other way to providing the periodicity condition.

Thus the family of oscillators (3.1) includes the two quite simple complementary asymptotics associated with the boundaries of the interval $1 \leq n < \infty$ as illustrated by Fig. 1.1. Respectively, there are two couples of periodic functions

$$\{x, \dot{x}\} = \{\sin t, \cos t\}, \quad \text{if } n = 1 \tag{3.4}$$

and

$$\{x, \dot{x}\} \to \{\tau(t), e(t)\}, \quad \text{if } n \to \infty \tag{3.5}$$

where $e(t) = \dot{\tau}(t)$ is a generalized derivative of the triangle wave, which is the square wave.[2]

Earlier, the power-form characteristics with integer exponents were employed for phenomenological modeling of the amplitude limiters of vibrating elastic structures [242] and illustrations of impact asymptotics [172, 176]. It should be noted that such phenomenological approaches to the modeling of impacts are designed to capture the integral effect of interaction with physical constraints while bypassing its local details near constraints. Such details obviously depend upon both the material properties of interacting bodies and physical conditions of interactions. In many cases, Hertz model of interaction is used to describe the local dynamics near constraint surfaces [84]. Note that direct replacement of the characteristic x^{2n-1} by the Hertzian restoring force $kx^{3/2}$ in (3.1) gives no oscillator. The equation,

$$\ddot{x} + kx^{3/2} = 0 \tag{3.6}$$

which is a particular case considered in [84], must be obviously accompanied by the condition $0 \leq x$, where $x = 0$ corresponds to the state at which the moving body and constraint barely touch each other with still zero interaction force.

The following modification brings system (3.6) into the class of oscillators with odd characteristics

$$\ddot{x} + k\text{sgn}(x)|x|^{3/2} = 0 \tag{3.7}$$

However, oscillator (3.7) essentially differs from oscillator (3.1) since Eq. (3.7) cannot describe any gap (clearance) in between the left and right constraint surfaces. In other words models (3.1) and (3.7) represent physically different situations. The gap 2Δ with its center at the origin, $x = 0$, can be introduced in Eq. (3.7) as follows:

$$\ddot{x} + k[H(x - \Delta)|x - \Delta|^{3/2} - H(-x - \Delta)|x + \Delta|^{3/2}] = 0 \tag{3.8}$$

where H is Heaviside unit-step function.

[2] The terms *triangular sine* and *rectangular cosine* can be also used to emphasize the choice for the initial time point, $\tau(0) = 0$ and $e(0) = 1$, and unit amplitudes.

This is a generalization of model (3.7), which is now derived from (3.8) by setting $\Delta = 0$. Equation (3.8) can be viewed as a physical impact oscillator that accounts for elastic properties of its components. As compared to phenomenological model (3.1), Eq. (3.8) was obtained on certain physical basis given by the Hertz contact theory.

Finally, oscillators with power-form characteristics, including their generalizations, can be found in physical literature [33, 78, 157], [80, 130] and different areas of applied mathematics and mechanics [5, 8, 9, 18, 45, 61, 67, 83, 113, 141, 142, 146, 207, 244]. In reference [195], the power-form restoring forces were introduced to simulate the liquid sloshing impacts; regarding this phenomenon, see also review article [90].

3.2 Nonlinear Oscillators Solvable in Elementary Functions

A class of strongly nonlinear oscillators admitting surprisingly simple exact general solutions at any level of the total energy is described below. Although the fact of exact solvability of these oscillators has been known for quite a long time [103], it did not attract much attention possibly due to the specific form of the oscillator characteristics with uncertain physical interpretations. It is clear however that, in a phenomenological way, such characteristics capture sufficiently general physical situations with hardening and softening behavior of the restoring forces. For instance, these oscillators were recently used as a phenomenological basis for describing different practically important physical and mechanical systems [53, 54, 158]. The hardening characteristic is close to linear for relatively small amplitudes but becomes infinity growing as the amplitude approaches certain limits. As a result, the corresponding temporal mode of vibration changes its shape from smooth quasi harmonic to the nonsmooth triangle wave of the rapidly growing frequency. In contrast, the softening characteristic behaves in a non-monotonic way such that the vibration shape is approaching the square wave as the amplitude is increasing. Earlier, amplitude-phase equations were obtained for a coupled array of the hardening oscillators [187]. It will be shown below that such oscillators admit explicit action-angle variables within the class of elementary functions. As a result, conventional averaging procedures become applicable to a wide range of nonlinear motions including transitions from high- to low-energy dynamics under small damping conditions. These solutions are in a good agreement with the corresponding numerical solutions at any energy level even within the first-order asymptotic approximation.

Hardening and softening cases of these oscillators are, respectively,

$$H = \frac{1}{2}(v^2 + \tan^2 x) \Rightarrow \ddot{x} + \frac{\tan x}{\cos^2 x} = 0 \tag{3.9}$$

and

$$H = \frac{1}{2}(v^2 + \tanh^2 x) \Rightarrow \ddot{x} + \frac{\tanh x}{\cosh^2 x} = 0 \tag{3.10}$$

where the mass is set to unity and thus $v = \dot{x}$ is interpreted as a generalized momentum of the Hamiltonian H, whereas x is a generalized coordinate.

Further objectives are to investigate the high-energy asymptotics with transitions to nonsmooth temporal mode shapes to show that both of the above oscillators can play the role of generating systems for regular perturbation procedures within the class of elementary functions.

Notice that oscillators (3.9) and (3.10) complement each other as those with stiff and soft characteristics represented in Fig. 3.1a and b, respectively. These oscillators can be represented also in the form

$$\ddot{x} + \tan x + \tan^3 x = 0 \tag{3.11}$$

$$\ddot{x} + \tanh x - \tanh^3 x = 0 \tag{3.12}$$

Further analyses of Eqs. (3.11) and (3.12) can be conducted by means of substitutions $q = \tan x$ and $q = \tanh x$, respectively. Interestingly enough, oscillators (3.11) and (3.12) without the cubic terms were considered by Timoshenko and Yang [232]. But, despite the simplified form, the corresponding solutions are expressed in terms of special functions.

3.2.1 Hardening Case

Consider first stiff oscillator (3.9), whose solution is

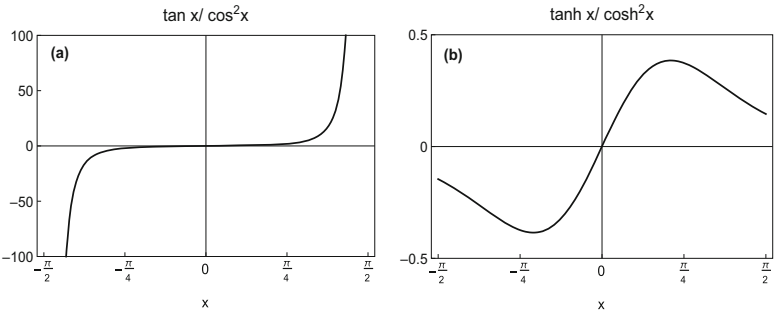

Fig. 3.1 Restoring force characteristics of exactly solvable strongly nonlinear oscillators (3.9) and (3.10): (**a**) hardening characteristic and (**b**) softening characteristic

$$x = \arcsin\left[\sin A \sin\left(\frac{t}{\cos A}\right)\right] \tag{3.13}$$

where A is an arbitrary constant, and another constant is introduced through the time shift $t- > t + const.$, since the equations admit the group of temporal shifts.

Therefore, function (3.13) represents a general periodic solution of the period $T = 2\pi \cos A$, while the total energy is expressed through the amplitude, A, as

$$E = \frac{1}{2}\tan^2 A \tag{3.14}$$

In zero energy limit, when the amplitude is close to zero, the oscillator linearizes, whereas solution (3.13) gives the corresponding sine-wave temporal shape. On the other hand, the energy becomes infinitely large as the parameter A approaches the upper limit $\pi/2$. In this case, the period vanishes while the oscillation takes the triangle wave shape as follows from expression (3.13). Figure 3.2a illustrates the evolution of the vibration shape as a function of phase, $\varphi = t/\cos A$, where $\alpha = \sin A$.

Action-Angle Variables

Below, the action-angle variables are introduced in terms of elementary functions. This enables one of considering non-periodic motions by using exact solution (3.13) as a starting point of the averaging procedure. For a single degree-of-freedom conservative oscillator, the action coordinate I is known to be the area bounded by the system path on the phase plane divided by 2π, whereas the angle φ coordinate is simply phase angle [16, 161, 164]. In the case of hardening restoring force characteristic (3.9), one obtains

$$I = \frac{1}{2\pi}\oint v dx = \frac{1}{\cos A} - 1 \tag{3.15}$$

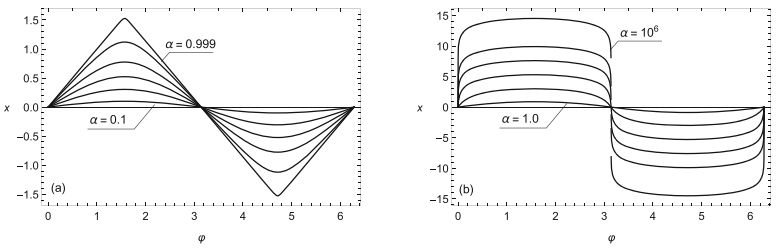

Fig. 3.2 Normalized temporal mode shapes of the oscillators with stiffening and softening restoring force characteristics in the displacement versus phase coordinates: (**a**) $x = \arcsin(\alpha \sin\varphi)$ and (**b**) $x = \text{arcsinh}(\alpha \sin\varphi)$

and

$$\varphi = \frac{t}{\cos A} \tag{3.16}$$

respectively.

The original coordinate and the velocity are expressed through the action-angle variables as follows:[3] [188]

$$x = \arcsin\left(\frac{\sqrt{2I + I^2}}{1 + I}\sin\varphi\right), \quad v = \frac{(1 + I)\sqrt{2I + I^2}\cos\varphi}{\sqrt{1 + \left(2I + I^2\right)\cos^2\varphi}} \tag{3.17}$$

To observe the convenience of action-angle coordinates, let us choose the Hamiltonian description of the oscillator. Taking into account expressions (3.14) and (3.15), and eliminating the amplitude A, gives the total energy and thus Hamiltonian

$$H = I + \frac{1}{2}I^2 \tag{3.18}$$

The corresponding differential equations of motion are derived as follows:

$$\dot{\varphi} = \frac{\partial H}{\partial I} = 1 + I, \quad \dot{I} = -\frac{\partial H}{\partial \varphi} = 0 \tag{3.19}$$

As it is seen, the oscillator is linearized with respect to the action-angle coordinates and hence possesses the exact general solution

$$I = I_0, \quad \varphi = (1 + I_0)\,t + \varphi_0 \tag{3.20}$$

where $I_0 > 0$ and φ_0 are arbitrary constants. By substituting (3.20) in (3.17), one can express the solution via the original coordinates. The meaning of the initial action is clear from the energy relationship

$$E = I_0 + \frac{1}{2}I_0^2 = \frac{1}{2}\tan^2 A \tag{3.21}$$

Note that the linearity of the Hamiltonian equations is due to the specific strongly nonlinear form of the coordinate transformation (3.17). *In other words, the system nonlinearity has been "absorbed" in a purely geometric way by the nonlinear coordinate transformation.*

As mentioned at the beginning, simplicity of the transformed system and that of the corresponding solution can be essentially employed for the purpose of

[3] The relationship for x was known earlier [164]. However, the complete set is required for nonconservative velocity-dependent perturbations.

perturbation analysis. Let us consider the differential equation of motion in the Newtonian form

$$\ddot{x} + \frac{\tan x}{\cos^2 x} = \varepsilon f\,(x, \dot{x}) \tag{3.22}$$

where ε is a small parameter.

This system is weakly nonconservative and therefore has no Hamiltonian. It is still possible nonetheless to consider expressions (3.17) as a transformation of state variables, $\{x, v\} \longrightarrow \{I, \varphi\}$. For that reason, let us represent equation (3.22) as a system of two first-order equations for the state variables, x and v,

$$\begin{aligned} \dot{x} &= v \\ \dot{v} &= -\frac{\tan x}{\cos^2 x} + \varepsilon f\,(x, v) \end{aligned} \tag{3.23}$$

Substituting (3.17) in (3.23) and then solving the system for $\dot{\varphi}$ and $\dot{I}$ give

$$\begin{aligned} \dot{\varphi} &= 1 + I - \frac{\varepsilon f(x, v) \sin\varphi}{(1 + I)\sqrt{\left(2I + I^2\right)\left[1 + \left(2I + I^2\right)\cos^2\varphi\right]}} \\ \dot{I} &= \frac{\varepsilon f(x, v)\sqrt{2I + I^2}\cos\varphi}{\sqrt{1 + \left(2I + I^2\right)\cos^2\varphi}} \end{aligned} \tag{3.24}$$

where the function $f(x, v)$ still must be expressed through the action-angle coordinates by means of (3.17).

Example of Linear Viscous Damping

In case of the linear damping, $f(x, v) \equiv -v$, Eqs. (3.24) take the form

$$\begin{aligned} \dot{\varphi} &= 1 + I + \frac{\varepsilon \cos\varphi \sin\varphi}{1 + \left(2I + I^2\right)\cos^2\varphi} \\ \dot{I} &= -\frac{\varepsilon\,(1 + I)\left(2I + I^2\right)\cos^2\varphi}{1 + \left(2I + I^2\right)\cos^2\varphi} \end{aligned} \tag{3.25}$$

Let us implement just one step of the averaging procedure and evaluate its effectiveness. Applying the operator of averaging with respect to the phase, φ, in (3.25) gives the corresponding first-order averaged system in the linear form

$$\dot{\varphi} = 1 + I, \quad \dot{I} = -\varepsilon I \tag{3.26}$$

Substituting the general solution of system (3.26) in (3.17) finally gives

$$x = \arcsin\left\{\frac{\sqrt{2I_0\exp(-\varepsilon t)+I_0^2\exp(-2\varepsilon t)}}{1+I_0\exp(-\varepsilon t)}\right. \\ \left.\times\sin\left[t+I_0\frac{1-\exp(-\varepsilon t)}{\varepsilon}+\varphi_0\right]\right\} \tag{3.27}$$

where I_0 and φ_0 are arbitrary constants. The corresponding time history records and phase plane diagrams for different damping coefficients are shown in Fig. 3.3. Even the leading order approximation appears to be in a good agreement with numerical solution for all the range of amplitudes. The analytical and numerical curves can be distinguished only at relatively large magnitudes of the damping parameter ε. Also, the graphs show that the temporal mode is gradually changing its shape from the triangular to harmonic as time increases and the amplitude decays.

Nonlinear Localized Damping

Let us consider the case of nonlinear damping

$$\ddot{x}+\frac{\tan x}{\cos^2 x}=-2\varepsilon\dot{x}\tan^2 x \tag{3.28}$$

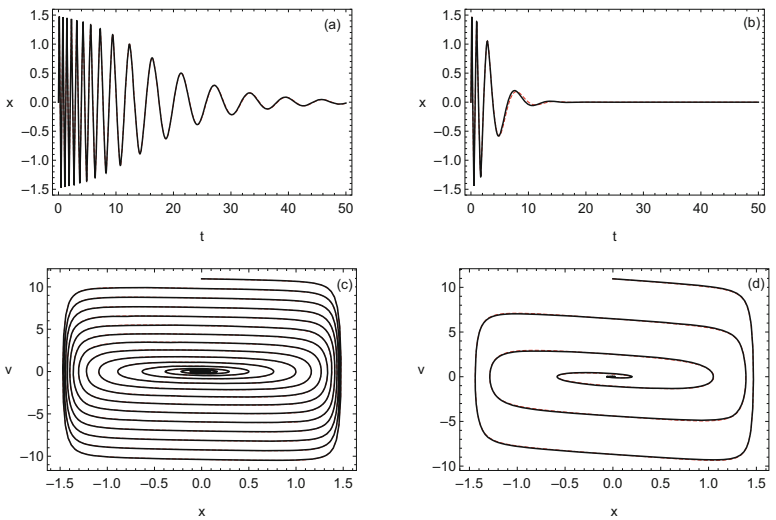

Fig. 3.3 The response of hardening oscillator (3.22) in case of the linear viscous damping, $f(x,v)\equiv -v$, under the initial conditions $I_0=10$ and $\varphi_0=0$, and two different damping parameters: $\varepsilon=0.2$ (**a**, **c**) and $\varepsilon=0.8$ (**b**, **d**); the numerical solution of the differential equation is represented for the time history (**a**, **b**) and phase plane diagrams (**c**, **d**) by the dashed curves

In this case, the perturbation is given by $f(x, v) \equiv -2v \tan^2 x$. Such a damping is rapidly growing near the boundaries of the interval $-\pi/2 \leq x \leq \pi/2$, but it becomes negligible when the amplitude is small, $|x| << 1$.

In the action-angle coordinates, first-order averaging gives

$$\dot{\varphi} = 1 + I, \quad \dot{I} = -\varepsilon I^2$$

and thus

$$\varphi = t + \frac{1}{\varepsilon} \ln(1 + \varepsilon I_0 t) + \varphi_0, \quad I = \frac{I_0}{1 + \varepsilon I_0 t}$$

Using the coordinate transformation (3.17) gives solution

$$x = \arcsin\left\{ \frac{\sqrt{I_0(2 + I_0 + 2\varepsilon I_0 t)}}{1 + I_0 + \varepsilon I_0 t} \sin\left[t + \frac{\ln(1 + \varepsilon I_0 t)}{\varepsilon} + \varphi_0 \right] \right\} \tag{3.29}$$

where I_0 and φ_0 are arbitrary constants.

Note that the amplitude decay of solutions (3.27) and (3.29) is qualitatively different. For instance, the amplitude of vibration (3.29) originally decays in a fast rate and then becomes very slow. In contrast, the amplitude of vibration (3.27) first decays slowly, and then the decay rate abruptly increases and then slows down again.

3.2.2 *Softening Case*

Let us consider now softening oscillator (3.10), whose exact solution is

$$x = \operatorname{arc\,sinh}\left[\sinh A \sin\left(\frac{t}{\cosh A} \right) \right] \tag{3.30}$$

Figure 3.2b shows that the temporal shape of high-energy vibrations approaches the square wave and thus essentially differs of that observed in the stiff case. To compare the shapes for different periods, the dependencies are given with respect to the phase variable $\varphi = t/\cosh A$ using the parameter $\alpha = \sinh A$. Based on solution (3.30), the action-angle coordinates are introduced as

$$x = \operatorname{arc\,sinh}\left(\frac{\sqrt{2I - I^2}}{1 - I} \sin\varphi \right), \quad v = \frac{(1 - I)\sqrt{2I - I^2}\cos\varphi}{\sqrt{1 - (2I - I^2)\cos^2\varphi}} \tag{3.31}$$

where the action is expressed through the parameter A as

$$I = 1 - \frac{1}{\cosh A} \tag{3.32}$$

All the analytical manipulations are analogous to those conducted for the stiff case. Taking into account (3.32) gives the total energy as a function of the action I

$$E = \frac{1}{2}\tanh^2 A = I - \frac{1}{2}I^2 \tag{3.33}$$

In the presence of the linear viscous damping,

$$\ddot{x} + \frac{\tanh x}{\cosh^2 x} = -\varepsilon \dot{x} \tag{3.34}$$

the averaging procedure gives the linear system

$$\dot{\varphi} = 1 - I, \quad \dot{I} = -\varepsilon I \tag{3.35}$$

which differs by sign in the first equation compared to system (3.26).

Integrating system (3.35) and substituting the result in (3.31) give general solution of the original equation

$$x = \operatorname{arc\,sinh}\left\{\frac{\sqrt{2I_0 \exp(-\varepsilon t) - I_0^2 \exp(-2\varepsilon t)}}{1 - I_0 \exp(-\varepsilon t)} \times \sin\left[t - I_0 \frac{1 - \exp(-\varepsilon t)}{\varepsilon} + \varphi_0\right]\right\} \tag{3.36}$$

The corresponding time history graphs and phase plane diagrams are shown in Fig. 3.4 for different damping coefficients. The leading order approximation appears to match the corresponding numerical solution for all range of amplitudes, unless the initial action I_0 approaches the magnitude 1. As follows from expressions (3.33), this magnitude corresponds to the maximum value of the total energy of the oscillator. Note that the energy of the hardening oscillator has no maximum.

3.3 Nonsmoothness Hidden in Smooth Processes

In this section, nonlinear beats phenomena are considered as another source of nonsmooth behavior that brings a certain physical meaning to oscillator (3.22). Note that nonlinear beats became of growing interest few decades ago from different viewpoints of physics and nonlinear dynamics [79, 112, 119, 131, 238]. Interestingly enough, phase variables of interacting oscillators with close natural frequencies may show nonsmoothness of temporal behavior during the beating [79], for instance,

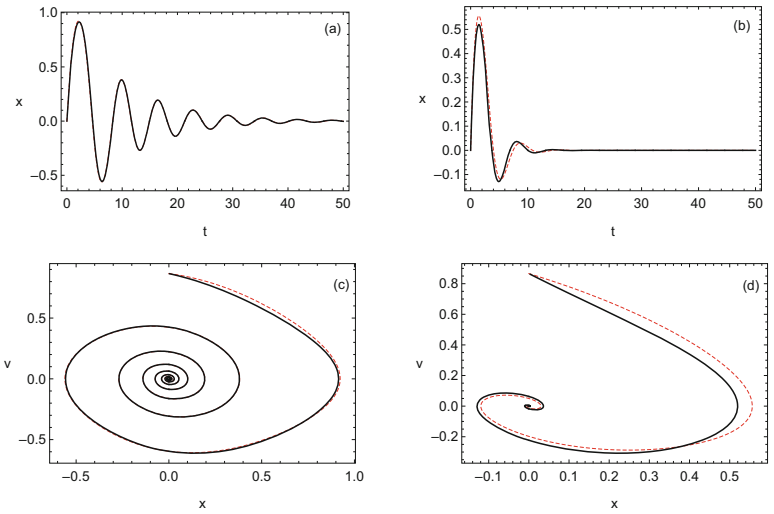

Fig. 3.4 The dynamics of the linearly damped softening oscillator under the initial conditions $I_0 = 0.5$, $\varphi_0 = 0$, and two different damping parameters: $\varepsilon = 0.2$ (**a**, **c**) and $\varepsilon = 0.8$ (**b**, **d**); numerical solution of the differential equation is represented for the time history (**a**, **b**) and phase plane diagrams (**c**, **d**) by the dashed curves

similar to that of a vibroimpact process [132, 133]. Such limiting dynamics were defined as a complementary nonstationary alternative to the normal mode motions. Below a new set of descriptive functions is introduced to analyze the beating effects directly in energy variables.

3.3.1 *Descriptive Functions for Interaction of Identical Oscillators*

Let us consider an ensemble of two identical harmonic oscillators with the natural frequency Ω:

$$\ddot{q}_k + \Omega^2 q_k = 0 \quad (k = 1, 2) \tag{3.37}$$

Although there is no interaction between oscillators (3.37) in terms of forces, there is still certain coupling through the time variable t. Namely, both oscillators have the same natural temporal scale $\delta = \Omega t$ with the same initial point. In other words two independent oscillators (3.37) still represent a system. Now let us denote $v_k = \dot{q}_k$ $(k = 1, 2)$ and then introduce symmetric 2×2 matrix

$$E_{kj} = \frac{1}{2}(v_k v_j + \Omega^2 q_k q_j) \tag{3.38}$$

and the following combinations of its elements [190]

$$\begin{aligned} E_{11} + E_{22} &= E \\ \frac{E_{11} - E_{22}}{E} &= P, \quad -1 \le P \le 1 \\ \frac{E_{12}}{\sqrt{E_{11}E_{22}}} &= Q, \quad -1 \le Q \le 1 \end{aligned} \tag{3.39}$$

where E is the total energy of both oscillators per unit mass and P is a unitless index characterizing the distribution of energy between the oscillators as

$$E_{11} = \frac{1}{2}E(1+P), \quad E_{22} = \frac{1}{2}E(1-P) \tag{3.40}$$

Relationships (3.40) are derived by solving the first two equations in (3.39) for E_{11} and E_{22}. To clarify the meaning of quantity Q and express the original state variables through E, P, and Q, let us assume that the oscillators are described by

$$q_1 = A_1 \cos\delta, \qquad q_2 = A_2 \cos(\delta + \Delta) \tag{3.41}$$

where $\delta = \Omega t$, A_1 and A_2 are constant amplitudes, and Δ is a phase shift. Then, substituting (3.41) in (3.38) gives

$$\begin{aligned} E_{12} &= \frac{1}{2}\Omega^2 A_1 A_2 [\sin\delta \sin(\delta+\Delta) + \cos\delta\cos(\delta+\Delta)] \\ &= \frac{1}{2}\Omega^2 A_1 A_2 \cos\Delta \\ E_{11}E_{22} &= \frac{1}{4}\Omega^4 A_1^2 A_2^2 \end{aligned} \tag{3.42}$$

Substituting (3.42) in (3.39) shows that the quantity Q represents the phase shift of oscillations as

$$Q = \frac{E_{12}}{\sqrt{E_{11}E_{22}}} = \cos\Delta \tag{3.43}$$

Now, substituting (3.41) in (3.40) and taking into account (3.38) give $\Omega^2 A_1^2 = E(1+P)$ and $\Omega^2 A_2^2 = E(1-P)$. Solving these equations for the amplitudes and taking into account (3.41) finally give the transformation from E, P, Δ, and δ back to the original state variables of both oscillators

$$\begin{aligned} q_1 &= \frac{1}{\Omega}\sqrt{E(1+P)}\cos\delta \\ v_1 &= -\sqrt{E(1+P)}\sin\delta \end{aligned}$$

$$q_2 = \frac{1}{\Omega}\sqrt{E(1-P)}\cos(\delta+\Delta) \qquad (3.44)$$
$$v_2 = -\sqrt{E(1-P)}\sin(\delta+\Delta)$$

Note that, in case of non-interacting linear oscillators (3.37), the quantities E, P, and Δ are constant. Therefore, in line with the idea of parameter variations and averaging, these can be assumed to be slowly varying functions under the presence of relatively small perturbations, such as coupling and nonlinearities. The advantage of such descriptive variables is due to their physical meaning given by (3.38) and (3.39). Also, in contrast to other types of characteristics, quantities (3.38) and (3.39) can be evaluated directly from numerical or experimental signals for state variables. However, the convenience of these variables becomes most obvious whenever the problem formulation deals with the effects of energy transfer or with the modal content of oscillations. In such cases, variables (3.39) reveal the necessary information in a straightforward way. For instance, as follows from (3.39) and confirmed by (3.44), the number $P = 0$ indicates the energy equipartition, $E_{11} = E_{22}$, whereas at $P = 1$ or $P = -1$ all the energy belongs to the first or to the second oscillator, respectively. Regarding the modal content, the numbers $Q = 1$ and $Q = -1$ correspond to the inphase ($\Delta = 0$) and antiphase ($\Delta = \pi$) vibration modes, respectively. In these cases, transformation (3.44) gives the corresponding couple of straight lines on configuration plane $q_1 - q_2$:

$$q_2 = \pm\sqrt{\frac{1-P}{1+P}}q_1 \qquad (3.45)$$

If $Q = 0$ ($\Delta = \pi/2$), then, according to (3.44), the system follows the elliptic path in either clockwise or counterclockwise direction:

$$\frac{q_1^2}{1+P} + \frac{q_2^2}{1-P} = \frac{E}{\Omega^2} \qquad (3.46)$$

Geometrical meaning of the *coherency index* Q is explained in Fig. 3.5. As already mentioned, in case of system (3.37), the numbers P and Q are fixed and can be determined from the initial conditions by means of relationships (3.38) and

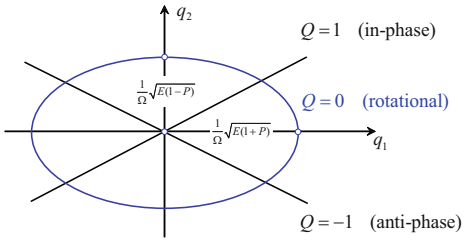

Fig. 3.5 Geometrical interpretation of the coherency index Q on the configuration plane

(3.39). In the general transient case, the temporal behavior of numbers P and Q reveals which of the above three modes is dominant during a certain time interval.

As noticed in Sect. 2.2.4, in physical literature, harmonic oscillations are often represented by rotating vectors on the complex plane. For that reason, let us express quantities (3.39) through the complex coordinates [120] $\psi_j = v_j + i\Omega q_j$, or inversely,

$$v_j = \frac{1}{2}\left(\psi_j + \bar{\psi}_j\right), \qquad q_j = \frac{1}{2i\Omega}\left(\psi_j - \bar{\psi}_j\right) \tag{3.47}$$

Substituting (3.47) in (3.38) gives

$$E_{kj} = \frac{1}{2}(v_k v_j + \Omega^2 q_k q_j) = \frac{1}{4}(\bar{\psi}_k \psi_j + \psi_k \bar{\psi}_j) \tag{3.48}$$

Hence the total energy of two oscillators excluding coupling, E, the energy distribution, P, and the index of coherency, Q, are calculated through the complex coordinates as:

$$E = E_{11} + E_{22} = \frac{1}{2}\left(\left|\psi_1\right|^2 + \left|\psi_2\right|^2\right) \tag{3.49}$$

$$P = \frac{E_{11} - E_{22}}{E_{11} + E_{22}} = \frac{\left|\psi_1\right|^2 - \left|\psi_2\right|^2}{\left|\psi_1\right|^2 + \left|\psi_2\right|^2}, \quad -1 \le P \le 1 \tag{3.50}$$

$$Q = \frac{E_{12}}{\sqrt{E_{11}E_{22}}} = \frac{\bar{\psi}_1\psi_2 + \psi_1\bar{\psi}_2}{2\left|\psi_1\right|\left|\psi_2\right|}, \quad -1 \le Q \le 1 \tag{3.51}$$

The example of analysis using these descriptive variables is considered in the next subsection.

3.3.2 *Systems with 1:1 Resonance*

Let us derive equations describing temporal behaviors of the new variables by considering a system of two interacting oscillators

$$\begin{aligned} \ddot{q}_1 + \Omega^2 q_1 + f_1(q_1, \dot{q}_1, q_2, \dot{q}_2) &= 0 \\ \ddot{q}_2 + \Omega^2 q_2 + f_2(q_1, \dot{q}_1, q_2, \dot{q}_2) &= 0 \end{aligned} \tag{3.52}$$

where the terms f_1 and f_2 are small enough to be viewed as perturbations.

In the state space, system (3.52) is represented in the form of four first-order differential equations

$$\begin{aligned}\dot{q}_1 &= v_1\\ \dot{v}_1 &= -\Omega^2 q_1 - f_1\\ \dot{q}_2 &= v_2\\ \dot{v}_2 &= -\Omega^2 q_2 - f_2\end{aligned} \tag{3.53}$$

where $f_k = f_k(q_1, v_1, q_2, v_2)$ $(k = 1, 2)$.

Due to the presence of perturbations, quantities (3.39) become time varying in a temporal rate dictated by the magnitude of perturbations, f_k, as follows from the derivative of the energy matrix

$$\frac{d}{dt}\begin{bmatrix} E_{11} & E_{12}\\ E_{21} & E_{22}\end{bmatrix} = -\frac{1}{2}\begin{bmatrix} 2f_1v_1 & f_1v_2 + f_2v_1\\ f_1v_2 + f_2v_1 & 2f_2v_2\end{bmatrix} \tag{3.54}$$

which is obtained from (3.38) by enforcing equations (3.53).

As noticed above, relationships (3.44) can be considered as a coordinate transformation in the system state space using the idea of parameter variations as

$$\{q_1, v_1, q_2, v_2\} \longrightarrow \{E(t), P(t), \Delta(t), \delta(t)\} \tag{3.55}$$

where E, P, and Δ are now slowly varying quantities, whose temporal rates are determined by the magnitude of terms f_1 and f_2 according to (3.54); recall expressions (3.39).

Note that, in the presence of perturbation, the time-dependent quantity E is losing its meaning of the system's total energy due to both possible nonconservative terms and the ignored energy of coupling. Nonetheless, under the assumption of small perturbation, the quantity E still can serve as a convenient estimate for the total excitation level of the system in line with the idea of Lyapunov functions.

Substituting (3.44) in (3.53) and solving the resultant equations for the derivatives of new state variables give

$$\begin{aligned}\frac{dE}{dt} &= \sqrt{E}\left[\sqrt{1-P}\,f_2\sin(\delta+\Delta) + \sqrt{1+P}\,f_1\sin\delta\right]\\ \frac{dP}{dt} &= -\frac{P}{\sqrt{E}}\left[\sqrt{1-P}\,f_2\sin(\delta+\Delta) + \sqrt{1+P}\,f_1\sin\delta\right]\\ &\quad -\frac{1}{\sqrt{E}}\left[\sqrt{1-P}\,f_2\sin(\delta+\Delta) - \sqrt{1+P}\,f_1\sin\delta\right]\\ \frac{d\Delta}{dt} &= \frac{1}{\sqrt{E}}\left[\frac{f_2\cos(\delta+\Delta)}{\sqrt{1-P}} - \frac{f_1\cos\delta}{\sqrt{1+P}}\right]\end{aligned} \tag{3.56}$$

and

$$\frac{d\delta}{dt} = \Omega + \frac{f_1 \cos\delta}{\sqrt{E(1+P)}} \tag{3.57}$$

where both functions f_1 and f_2 must be expressed through E, P, Δ and δ by means of (3.44).

At this point, Eqs. (3.56) and (3.57) still represent the exact equivalent of original system (3.53). Further, assuming that $f_k \sim \varepsilon$ $(0 < \varepsilon << 1, k = 1, 2)$, different procedures of asymptotic integration can be applied to system (3.56) and (3.57). Practically acceptable approximate solutions can be often obtained by the direct one-step averaging of the right-hand side of system (3.56) and (3.57) with respect to the fast phase δ over the period 2π by means of the integral operator

$$< \cdots >_\delta = \frac{1}{2\pi}\int_0^{2\pi} \cdots d\delta \tag{3.58}$$

Energy Localization in Coupled Identical Duffing Oscillators

Let us consider the example of two coupled Duffing oscillators by assuming

$$\begin{aligned} f_1 &= 2\zeta\Omega v_1 + \beta(q_1 - q_2) + \alpha q_1^3 \\ f_2 &= 2\zeta\Omega v_2 + \beta(q_2 - q_1) + \alpha q_2^3 \end{aligned} \tag{3.59}$$

Substituting (3.59) in (3.56) and (3.57), taking into account (3.44), and applying averaging (3.58) to the right-hand side of the resultant system give

$$\begin{aligned} \frac{dE}{dt} &= -2\zeta\Omega E \\ \frac{dP}{dt} &= \frac{\beta}{\Omega}\sqrt{1-P^2}\sin\Delta \\ \frac{d\Delta}{dt} &= -\frac{3\alpha}{4\Omega^3}EP - \frac{\beta\cos\Delta}{\Omega\sqrt{1-P^2}}P \end{aligned} \tag{3.60}$$

and

$$\frac{d\delta}{dt} = \Omega + \frac{3\alpha}{8\Omega^3}E(1+P) + \frac{\beta}{2\Omega}\left(1 - \sqrt{\frac{1-P}{1+P}}\cos\Delta\right) \tag{3.61}$$

Let us introduce new temporal argument $\bar{t}$ and the total excitation level $\kappa(\bar{t})$ as

$$t = \frac{\Omega}{\beta}\bar{t}, \qquad E(t) = \frac{4\beta\Omega^2}{3\alpha}\kappa(\bar{t}) \tag{3.62}$$

Substituting (3.62) in (3.60) and solving the first equation for κ bring the averaged system to the form

$$\begin{aligned} \kappa &= \kappa_0 \exp\left(-2\frac{\zeta}{\beta}\Omega^2 \bar{t}\right) \\ \frac{dP}{d\bar{t}} &= -\frac{\partial H}{\partial \Delta} = \sqrt{1-P^2}\sin\Delta \\ \frac{d\Delta}{d\bar{t}} &= \frac{\partial H}{\partial P} = -P\left(\kappa + \frac{\cos\Delta}{\sqrt{1-P^2}}\right) \end{aligned} \tag{3.63}$$

where $\kappa_0 = \kappa(0)$ and

$$H = H(P, \Delta, \bar{t}) = -\frac{1}{2}\kappa(\bar{t})P^2 + \sqrt{1-P^2}\cos\Delta \tag{3.64}$$

It is seen that P and Δ can play the role of Hamiltonian generalized momentum and generalized coordinate, respectively. Note that the Hamiltonian structure occurs despite the presence of dissipation in the original system. Obviously, Hamiltonian (3.64) is not conserved, unless $\zeta = 0$, and thus, enforcing system (3.63) gives

$$\frac{dH}{d\bar{t}} = \frac{\zeta}{\beta}\Omega^2 P^2 \kappa \tag{3.65}$$

Thus it is found that the resonance energy flow between the two interacting oscillators is described with an effective Hamiltonian oscillator. In order to consider the oscillatory dynamics, the damping ratio ζ will be assumed to be small enough to have the adiabatic effect on system (3.63). This system therefore can be viewed as a dynamical system on the phase plane $\Delta - P$ whose phase flow depends upon the total excitation level, κ. Since the right-hand side of system (3.63) is 2π-periodic with respect to Δ, it is sufficient to investigate two cells of the phase portrait including the stationary points $(\Delta, P) = (0, 0)$ and $(\Delta, P) = (\pi, 0)$, corresponding to the inphase and antiphase modes, respectively. As follows from the right-hand side of (3.63), the inphase mode is unique at any positive κ, whereas the antiphase mode can bifurcate to give rise for two new modes, when the total excitation level κ exceeds the critical level

$$\kappa^* = 1 \Longrightarrow E^* = \frac{4\beta\Omega^2}{3\alpha} \tag{3.66}$$

The corresponding stationary points are given by

$$(\Delta, P) = (0, \pm\sqrt{1-\kappa^{-2}}), \qquad 1 \le \kappa \tag{3.67}$$

Both critical and supercritical phase portraits are shown in Fig. 3.6a and b, respectively. These illustrate the bifurcation of the antiphase stationary point from

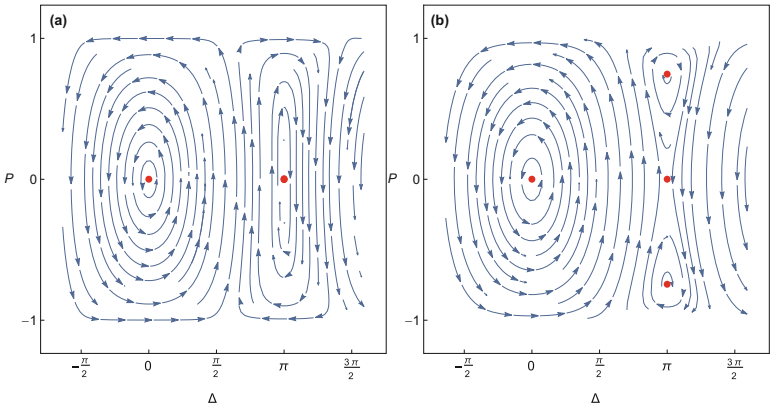

Fig. 3.6 Phase portraits of system (3.63) at fixed excitation levels: (**a**) $\kappa = 1$—critical, (**b**) $\kappa = 1.5$—supercritical

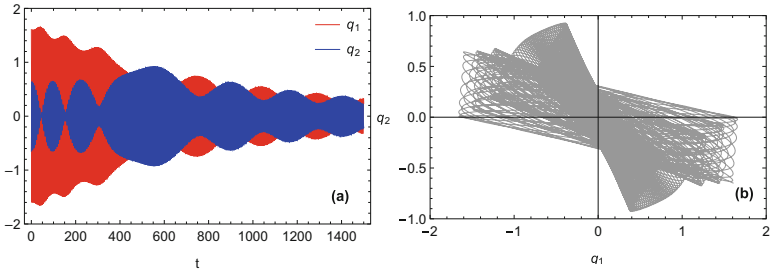

Fig. 3.7 Transition from local to antiphase mode due to the adiabatic energy loss: (**a**) time history response and (**b**) configuration plane under the following parameters and initial conditions: $\Omega = 1.0$, $\zeta = 0.001$, $\alpha = 0.08$, $\beta = 0.03$, $E(0) = 1.5$ ($\kappa(0) = 3.0$), $P(0) = 0.72$, $\Delta(0) = \pi - 0.001$

center to saddle and two centers, creating two local modes. Such effects are usually referred to as the symmetry breaking bifurcation in a perfectly symmetric system leading to the possibility of energy localization. As follows from (3.67), the energy localization/trapping effect can occur on a high-energy level. Assuming that the model remains adequate as the energy is increasing, one can reach the limit in which all the energy becomes localized at just one of the two oscillators

$$(\Delta, P) \sim (0, \pm 1), \qquad 1 \ll \kappa \tag{3.68}$$

Practically however, if no energy inflow is maintained, the dissipation effect will cause a gradual decrease of the quantity κ. As a result, the local modes will eventually disappear followed by the reciprocal beatwise oscillations as seen from Figs. 3.7 and 3.8.

Let us consider the conservative system, $\zeta = 0$, when κ is a fixed number. In this case, as follows from (3.65), system (3.63) admits the following integral:

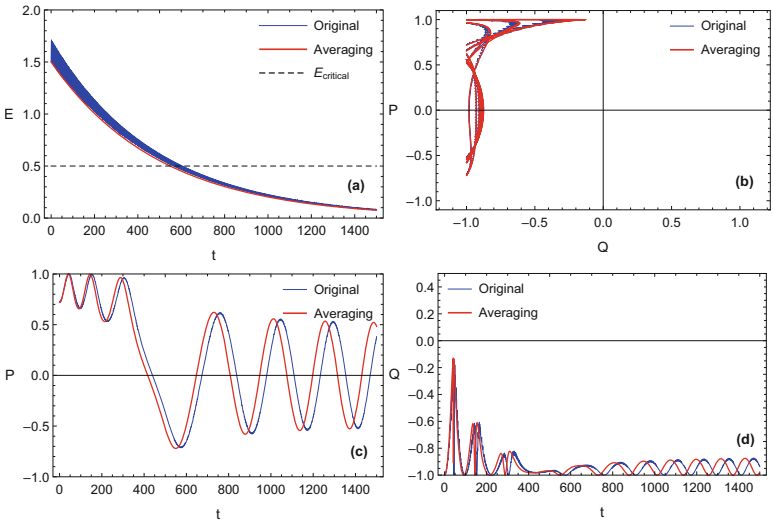

Fig. 3.8 Illustration of the delocalization process (Fig. 3.7) in terms of the variables $\{E, P, Q\}$ obtained from numerical solutions of the original and averaged systems in comparison: (**a**) total excitation level, (**b**) $P - Q$ diagram, (**c**) the evolution of energy distribution, and (**d**) coherency index

$$H(P, \Delta) = H_0 = H(P, \Delta)|_{\tilde{t}=0} \tag{3.69}$$

Substituting $P = \sin\phi$ $(-\pi/2 \le \phi \le \pi/2)$ in (3.63) and (3.69) and then eliminating the phase shift Δ give a strongly nonlinear conservative oscillator for the new variable ϕ describing the resonance beatwise energy flow

$$\frac{d^2\phi}{d\tilde{t}^2} + \left(H_0 + \frac{1}{2}\kappa\right)^2 \frac{\tan\phi}{\cos^2\phi} - \frac{1}{8}\kappa^2 \sin 2\phi = 0 \tag{3.70}$$

where H_0 is expressed through the parameter κ and initial angles ϕ_0 and Δ_0 as

$$H_0 = -\frac{1}{2}\kappa \sin^2\phi_0 + \cos\phi_0 \cos\Delta_0, \qquad \kappa = \frac{3\alpha E}{4\beta\Omega^2} \tag{3.71}$$

Oscillator (3.70) has the effective potential energy described by

$$V(\phi) = \frac{1}{2}\left(H_0 + \frac{1}{2}\kappa\right)^2 \tan^2\phi - \frac{1}{8}\kappa^2 \sin^2\phi \tag{3.72}$$

Note that using oscillator (3.70) is complicated by the fact that the number H_0 depends upon the initial conditions given by

$$\sin\phi_0 = P_0, \qquad \left.\frac{d\phi}{d\bar{t}}\right|_{\bar{t}=0} = \sin\Delta_0 \tag{3.73}$$

where the second relationships follow from (3.63).

Hidden Nonsmooth Effects in Weakly Coupled Harmonic Oscillators

It follows from (3.62) that the parameter κ takes zero value if the original system (3.52) and (3.59) is linear, $\alpha = 0$. In this case oscillator (3.70) has exact analytical solution in terms of elementary functions

$$\phi = \arcsin\left[\sin\phi_0 \sin\left(|\cos\Delta_0|\bar{t} + \frac{\pi}{2}\right)\right] \tag{3.74}$$

In this case, the energy distribution, $P = \sin\phi$, behaves as a harmonic oscillator according to the sine wave law

$$P = P_0 \sin\left(|\cos\Delta_0|\bar{t} + \frac{\pi}{2}\right) \tag{3.75}$$

where $P_0 = \sin\phi_0$ is the initial energy distribution.

The phase ϕ behaves in a quite different way. As discussed briefly in Sect. 1.2.4, solution (3.74) admits two simple limits, such as the sine wave

$$\phi \sim \phi_0 \sin\left(|\cos\Delta_0|\bar{t} + \frac{\pi}{2}\right), \quad |P_0| \ll 1 \tag{3.76}$$

and the triangle wave

$$\phi \sim \frac{\pi}{2}\tau\left(\frac{2}{\pi}|\cos\Delta_0|\bar{t} + 1\right), \quad |P_0| \sim 1 \tag{3.77}$$

Figure 3.9 illustrates temporal mode shapes of the phase variables ϕ and Δ at different parameter of total excitation values κ. The initial distribution is close to predominantly one of the two oscillators, $P(0) \sim 1$. It is seen that such an uneven initial distribution results in oscillations of the angle ϕ within almost its entire interval $(-\pi/2, \pi/2)$ with a close to the triangle wave shape described by (3.77).

As mentioned in the preamble to this section, the most intensive energy exchange between subsystems can be viewed as a logical alternative to the stationary case with no energy exchange at all. Since the latter case associates with the normal mode motions, such alternative provides an adequate asymptotic limit for interpretations of different physical effects that cannot be described with conventional normal mode expansions.

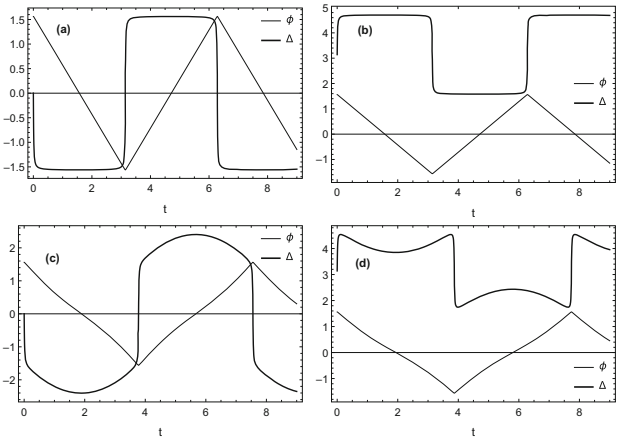

Fig. 3.9 Temporal shapes of the phase variables at $P(0) \sim 1$ ($\phi_0 = \pi/2 - 0.01$): (**a**) $\kappa = 0$, $\Delta = -0.001$, (**b**) $\kappa = 0$, $\Delta = \pi - 0.001$, (**c**) $\kappa = 1.5$, $\Delta = -0.001$, and (**d**) $\kappa = 1.5$, $\Delta = \pi - 0.001$

3.3.3 Energy Exchange Oscillator

As shown in Sect. 3.3.1, the energy exchange strongly nonlinear oscillator (3.70) admits the exact solution in terms of elementary functions, if the original system is linear, $\kappa = 0$. Now let us apply the methodology of Sect. 3.2 to the case $\kappa \neq 0$, when exact analytical solution cannot be expressed through elementary functions. First, let us represent the oscillator (3.70) in the following form:

$$\frac{d^2\phi}{dp^2} + \frac{\tan\phi}{\cos^2\phi} = \mu \sin 2\phi \tag{3.78}$$

where $p = |H_0 + \kappa/2|\,\bar{t}$ is a new temporal argument, whose parameters H_0 and κ are defined in (3.71), and

$$\mu = \frac{1}{2}\frac{\kappa^2}{(2H_0 + \kappa)^2} = \frac{1}{2}\frac{\kappa^2}{(\kappa\cos^2\phi_0 + 2\cos\phi_0\cos\Delta_0)^2} \tag{3.79}$$

The corresponding initial conditions can be obtained from (3.73) by taking into account the temporal substitution $p \to \bar{t}$. There are two possible ways to asymptotic simplifications of the essentially nonlinear equation (3.78).

Asymptotic of Equipartition

The first way is using the assumption that the initial energy is distributed almost equally between the oscillators of the ensemble (3.52), namely $|P_0| << 1$ or

$|\phi_0| << 1$. In this case, Eq. (3.78) can be reduced to the following Duffing equation:

$$\frac{d^2\phi}{dp^2} + (1-2\mu)\phi + \frac{4}{3}(1+\mu)\phi^3 = 0 \tag{3.80}$$

When $\mu < 1/2$, Eq. (3.80) describes periodic energy exchange. The period of the energy exchange process is given by the corresponding solution of Duffing equation (3.80). However, the point $(\phi, d\phi/dp) = (0,0)$ on the phase plane of oscillator (3.80) is changing its type from center to saddle when

$$\mu > \frac{1}{2} = \mu^* \tag{3.81}$$

Note that the critical number $\mu = \mu^*$ makes sense only for the neighborhood of antiphase mode (see Fig. 3.6b) as follows from relationship (3.79) after the following substitutions:

$$\mu|_{\{\Delta_0=\pi,\phi_0=0\}} = \frac{1}{2}\frac{\kappa^2}{(\kappa-2)^2} \tag{3.82}$$

$$\mu|_{\{\Delta_0=0,\phi_0=0\}} = \frac{1}{2}\frac{\kappa^2}{(\kappa+2)^2} \tag{3.83}$$

It is seen that formula (3.82) gives μ^* at $\kappa = \kappa^*$, whereas (3.83) gives μ, which is below μ^* at any positive κ.

Phase trajectories of oscillator (3.78) are shown in Fig. 3.10 for both critical and supercritical numbers μ. In order to keep μ fixed on the entire family of trajectories, we have to admit different κ on different trajectories. In particular, the numbers κ in Fig. 3.10 are obtained by substituting the fixed initial phase $\Delta_0 = \pi$ and different initial ϕ_0 in the inverse of (3.79)

$$\kappa = \frac{8(\sqrt{2\mu}\cos\phi_0 - 2\mu\cos^3\phi_0)\cos\Delta_0}{4\mu\cos 2\phi_0 + \mu\cos 4\phi_0 + 3\mu - 4} \tag{3.84}$$

The transition in phase diagrams of Fig. 3.10 is similar to that in Fig. 3.6 near the antiphase mode, except for different meaning and orientation of axes.

Low-Energy-Intensive Beats

The second way of asymptotic simplification of Eq. (3.78) is less conventional. We skip the condition $|\phi_0| << 1$ by allowing the energy to be distributed in any proportion while assuming that μ is sufficiently small. As follows from (3.79) and (3.71), the condition of small μ requires the quantity $\kappa = 3\alpha E/(4\beta\Omega^2)$ to be small. When $\mu \to 0$, the equation of energy exchange oscillator (3.78) still remains

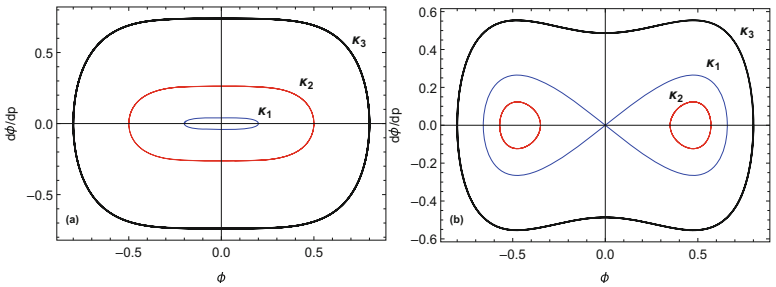

Fig. 3.10 Phase trajectories of the energy exchange oscillator: (**a**) $\mu = 1/2$—critical, $\kappa_1 = 0.999797$, $\kappa_2 = 0.991534$, $\kappa_3 = 0.938073$, and (**b**) $\mu = 0.8$—supercritical, $\kappa_1 = 1.11696$, $\kappa_2 = 1.12299$, $\kappa_3 = 1.09204$

strongly nonlinear but becomes exactly solvable in elementary functions. To employ this fact, let us introduce action-angle variables as described in Sect. 3.2

$$\phi = \arcsin\left(\frac{\sqrt{2I + I^2}}{1 + I}\sin\varphi\right)$$
$$v = \frac{(1 + I)\sqrt{2I + I^2}\cos\varphi}{\sqrt{1 + \left(2I + I^2\right)\cos^2\varphi}} \tag{3.85}$$

Following the procedure of Sect. 3.2 gives still exact equivalent of oscillator (3.78) in action-angle variables

$$\frac{dI}{dp} = \mu\frac{I(2 + I)}{(1 + I)^2}\sin 2\varphi$$
$$\frac{d\varphi}{dp} = 1 + I - \frac{2\mu}{(1 + I)^3}\sin^2\varphi \tag{3.86}$$

A direct averaging with respect to the phase φ can be applied to the right-hand side of system (3.86) to obtain the averaged system in the leading order approximation

$$\frac{dI}{dp} = 0, \qquad \frac{d\varphi}{dp} = 1 + I - \frac{\mu}{(1 + I)^3} \tag{3.87}$$

and its solution as

$$I = I_0 = const., \qquad \varphi = \left[1 + I_0 - \frac{\mu}{(1 + I_0)^3}\right]p \tag{3.88}$$

Substituting (3.88) in (3.85) gives the corresponding relationships in terms of the original variables.

High-order approximations can be obtained with canonical transformations of the Hamiltonian of oscillator (3.78). Such Hamiltonian can be expressed through the action-angle variables (3.85) as

$$H_\phi(I,\varphi,\mu)=\frac{1}{2}I(I+2)+\mu\frac{1+I(I+2)\cos 2\varphi}{2(I+1)^2} \tag{3.89}$$

Obviously, Eqs. (3.86) now follow from the Hamiltonian equations

$$\frac{dI}{dp}=-\frac{\partial H_\phi}{\partial\varphi},\qquad \frac{d\varphi}{dp}=\frac{\partial H_\phi}{\partial I} \tag{3.90}$$

Recall that $\{I,\varphi\}$ represent the action-angle variables of oscillator (3.78) only for the unperturbed case, $\mu=0$. This is why the angle φ is still present in Hamiltonian (3.89) although through the term of order μ. A high-order averaging can be implemented as a canonical transformation $\{I,\varphi\}\to\{J,\psi\}$ eliminating the fast phase from Hamiltonian (3.89). The main advantage of the Hamiltonian approach is that, instead of manipulating differential equations (3.90), the procedure deals with just one descriptive function $H_\phi(I,\varphi,\mu)$. In the leading order, the corresponding variable transformation must be identical since Hamiltonian (3.89) already has no fast phase at $\mu=0$. Using the automatic system of symbolic manipulations *Mathematica*$^{(R)}$ gives the transformation in the first asymptotic order as

$$\begin{aligned} I&=J-\mu\frac{J(2+J)}{2(1+J)^3}\cos 2\psi+O(\mu^2)\\ \varphi&=\psi-\mu\frac{J^2+2J-2}{4(1+J)^4}\sin 2\psi+O(\mu^2)\end{aligned} \tag{3.91}$$

This transformation brings Hamiltonian (3.89) to the form with no fast phase in the first-order of μ

$$H_\phi\to H_\psi=\frac{1}{2}J(J+2)+\frac{\mu}{2(1+J)^2}+O(\mu^2) \tag{3.92}$$

As a result, the new system takes the form, which is similar to (3.87) with the error of order $O(\mu^2)$

$$\frac{dJ}{dp}=-\frac{\partial H_\psi}{\partial\psi}=O(\mu^2),\qquad \frac{d\psi}{dp}=\frac{\partial H_\psi}{\partial J}=1+J-\frac{\mu}{(1+J)^3}+O(\mu^2) \tag{3.93}$$

Also, the form of solution for the fast phase is similar to (3.88)

$$J = J_0, \qquad \psi = \left[1 + J_0 - \frac{\mu}{(1+J_0)^3}\right] p \tag{3.94}$$

where $J_0 = const$. The inverse transformation to the original variables $\{\phi, v\}$ becomes more complicated than (3.85) due to the extra step according to (3.91).

3.3.4 Interaction of Liquid Sloshing Modes

The terminology of liquid sloshing covers both the physics of sloshing dynamics and the related mathematical methods [1, 57, 87, 90]. Many finite degrees-of-freedom sloshing models are obtained by representing the free liquid surface, say $\eta = \eta(t, x, y)$ (see Fig. 3.11), as a linear combination of some modal functions $\{U_k(x, y)\}$ with unknown time-dependent amplitudes

$$\eta(t, x, y) = \sum_k q_k(t) U_k(x, y) \tag{3.95}$$

Then applying Galerkin or similar method gives a set of ordinary differential equations for the amplitudes $\{q_k(t)\}$. The modal functions often represent a mathematically convenient orthogonal basis obtained as eigen functions of the corresponding linearized model of zero-viscosity fluid. Although such modal functions are conventionally called (linear) *sloshing modes*, in reality, physical sloshing modes may appear to be quite different due to viscous and nonlinear coupling effects. The sloshing waves observed in experiments usually associate with some stationary solutions of the entire nonlinear system for the modal amplitudes $\{q_k(t)\}$ and thus may combine two or even more predominant *linear sloshing modes* (LSMs). Since nonlinearity is essential for determining such combinations, the term *nonlinear sloshing modes* (NSMs) is meant in the present text. Below we follow reference [190], where the equations for modal amplitudes derived in [93] are used. Note that details of such derivations from the fluid dynamic equations are technically complicated and somewhat irrelevant to the present content. The model assumes irrotational flows of incompressible and originally inviscid fluid inside the tank with perfectly stiff walls. The tank has a square base whose side length is unity, $w = l = 1$, so that the fluid depth h is measured in the units of side wall length as shown in Fig. 3.11. On one hand, the assumption of square base brings formal simplifications to the governing differential equations of motion. On the other hand, the symmetry-induced 1:1 resonance coupling between the first two dominating modes essentially complicates the system dynamics, since the linear superposition principle does not hold in nonlinear cases.

A reasonable modal reduction therefore must include couples of symmetric modes, for instance,

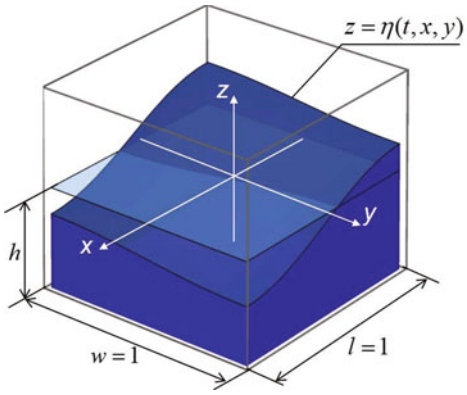

Fig. 3.11 Liquid sloshing in square tank

$$\eta(t, x, y) = q_1(t) \sin \pi x + q_2(t) \sin \pi y \tag{3.96}$$

Due to the perfect symmetry of square base, the first two modes satisfy exactly the 1:1 resonance condition $\Omega_1 = \Omega_2 \equiv \Omega$, and the corresponding differential equations of motion take the symmetric form

$$\begin{aligned} \ddot{q}_1 + 2\zeta\Omega\dot{q}_1 + \Omega^2 q_1 + f(q_1, q_2, \dot{q}_1, \dot{q}_2) &= 0 \\ \ddot{q}_2 + 2\zeta\Omega\dot{q}_2 + \Omega^2 q_2 + f(q_2, q_1, \dot{q}_2, \dot{q}_1) &= 0 \end{aligned} \tag{3.97}$$

where the phenomenological damping ratios are assumed to be the same, $\zeta = 0.0005$, and the nonlinear terms are given by the polynomial derived in [92]

$$f(q_1, q_2, \dot{q}_1, \dot{q}_2) \equiv S_3 q_1 \dot{q}_1{}^2 + S_4 q_1 \dot{q}_2{}^2 + S_5 q_2 \dot{q}_1 \dot{q}_2 + S_8 q_1{}^3 + S_9 q_1 q_2{}^2 \tag{3.98}$$

The quantities $S_i (i = 3, 4, 5, 8, 9)$ depend upon the tank depth h assuming that other dimensions are unity as shown in Fig. 3.11. In particular, $S_3 = 2.46654$, $S_4 = 4.9348$, $S_5 = -1.94182$, $S_8 = -2.53216$, and $S_9 = -1.05117$, when $h = 0.45$. Note also that, in references [92] and [190], the equations are scaled in such a way that $\Omega = 1$.

To bridge (3.97) with the standard form (3.53) of Sect. 3.3.1, let us set

$$f_1 = 2\zeta\Omega v_1 + f(q_1, q_2, v_1, v_2), \qquad f_2 = 2\zeta\Omega v_2 + f(q_2, q_1, v_2, v_1) \tag{3.99}$$

Then applying the averaging procedure of Sect. 3.3.1 gives equations[4]

[4] Note that, in reference [190], the origin $\Delta = 0$ corresponds to the antiphase mode. Therefore, transformation (3.44) must be adapted with the phase shift $\Delta \to \Delta + \pi$ in order to match the version used in [190]; Eqs. (3.100) and (3.101) still remain the same.

$$\begin{aligned}\frac{dE}{dt} &= -2\zeta\Omega E\\ \frac{dP}{dt} &= A\left(1-P^2\right)\sin 2\Delta\\ \frac{d\Delta}{dt} &= P(B-A\cos 2\Delta)\end{aligned} \tag{3.100}$$

and

$$\frac{d\delta}{dt} = \Omega + \frac{1}{2}[C - BP - A(1-P)\cos 2\Delta] \tag{3.101}$$

where A, B, and C are time-dependent quantities proportional to the total excitation level $E = E(t)$:

$$\begin{aligned}A = A(t) &= \frac{E(t)}{4\Omega^3}[\Omega^2(S_4 - S_5) - S_9]\\ B = B(t) &= \frac{E(t)}{4\Omega^3}[\Omega^2(-S_3 + 2S_4) - 3S_8 + 2S_9]\\ C = C(t) &= \frac{E(t)}{4\Omega^3}[\Omega^2(S_3 + 2S_4) + 3S_8 + 2S_9]\end{aligned} \tag{3.102}$$

The first equation in (3.100) describes the exponential energy decay of the first two modes combined:

$$E(t) = E(0)\exp(-2\zeta\Omega t) \tag{3.103}$$

The fast phase δ, described by the last equation in (3.100), determines the principal temporal scale, which is usually of little interest. Any way, Eq. (3.101) is solved for $\delta(t)$ by the direct integration as soon as the functions $P(t)$ and $\Delta(t)$ are known. As follows from (3.102), all the coefficients of the second and third equations in (3.100) decay with the same time rate according to (3.103). As a result, one can introduce a variable temporal scale, say $s(t)$, associated with the rate of energy dissipation. The corresponding function is given by the differential equation $ds(t) = A(t)dt$ under the initial condition $s(0) = 0$ as follows

$$s = A(0)\int_0^t \exp(-2\zeta\Omega t)dt = \frac{A(0)}{2\zeta\Omega}[1 - \exp(-2\zeta\Omega t)] \tag{3.104}$$

Now assuming that $P = P(s)$ and $\Delta = \Delta(s)$ and applying the substitution $t \to s$ as $d/dt = A\, d/ds$ brings system (3.100) to the effective Hamiltonian form for the couple of conjugate variables $\{\Delta, P\}$

$$\frac{dP}{ds} = -\frac{\partial H}{\partial \Delta} \equiv \left(1-P^2\right)\sin 2\Delta$$

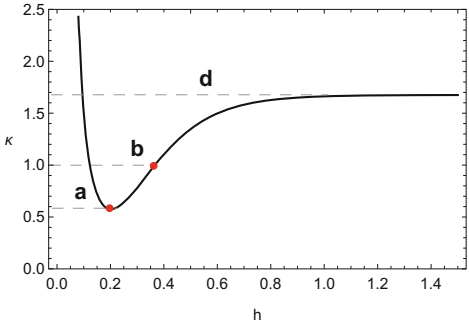

Fig. 3.12 The dependence of parameter κ versus fluid depth for the square tank, $w = l = 1$, based on the data of reference [91]: (**a**) minimum; (**b**) critical value; and (**d**) asymptotic maximum

$$\frac{d\Delta}{ds} = \frac{\partial H}{\partial P} \equiv (\kappa - \cos 2\Delta) P \tag{3.105}$$

with Hamiltonian,

$$H = H(P, \Delta) \equiv \frac{1}{2}\kappa P^2 + \frac{1}{2}\left(1 - P^2\right)\cos 2\Delta \tag{3.106}$$

where $\kappa = B/A$ is a constant parameter linked to the tank geometry namely the fluid depth as shown in Fig. 3.12.

The physical meaning of this result is that the energy level of sloshing has no effect on the resonance dynamics except for the slowing down of their temporal scale. From the mathematical standpoint, this is explained by the form of nonlinearity in (3.98). Since the polynomial f is *homogeneous*, $f(\lambda q_1, \lambda q_2, \lambda \dot{q}_1, \lambda \dot{q}_2) = \lambda^3 f(q_1, q_2, \dot{q}_1, \dot{q}_2)$, all the proportions between different terms of such polynomials remain fixed regardless of the amplitude levels λ. As follows from (3.105), κ is a single parameter of the effective oscillator.

The phase plane diagrams of system (3.105) represent level lines of the Hamiltonian $H = H(P, \Delta)$ versus the parameter κ and are shown in Fig. 3.13. The major qualitative transition takes place when $\kappa = 1$. Namely, the two cells I and A, surrounding the stationary Points (centers), collapse into vertical lines by giving rise two saddle points. This transition is accompanied by developing phase channels near the upper and lower cell boundaries $P = \pm 1$. In terms of NSMs, both inphase and antiphase NSMs become unstable, while only circular/rotational modes remain; see Fig. 3.5 for interpretation on the configuration plane $q_1 - q_2$. Compared to the case of linear elastic coupling of identical oscillators, which is represented by Fig. 3.6, the period of phase portrait along the coordinate Δ is shorter as many as twice. This follows also from the comparison of effective Hamiltonians (3.64) and (3.106). The reason is that the inphase and antiphase sloshing modes are physically equivalent due to the symmetry of square tank with respect to both its diagonals. As a result, system (3.97) admits either of the two replacements $q_1 \to -q_1$ or $q_2 \to -q_2$. In case of a mass-spring system with elastic coupling, the antiphase mode is carrying

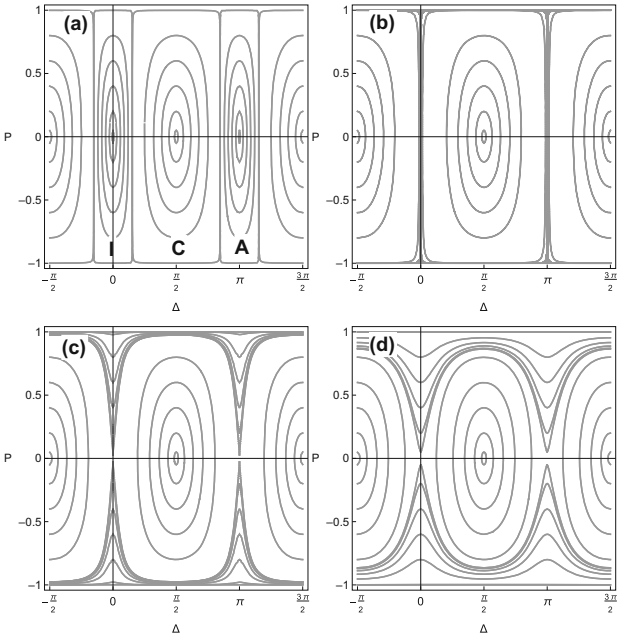

Fig. 3.13 Phase plane $\Delta - P$ diagrams of the effective Hamiltonian system at different κ: (**a**) $\kappa = 0.5753$—minimum reached at $h = 0.20156$, C—cells of circular modes, I—cells of inphase mode, and A—cells of antiphase mode; (**b**) $\kappa = 1.0$—critical value reached at $h = 0.3666$; (**c**) $\kappa = 1.1$—slightly supercritical value reached at $h = 0.3992$; (**d**) $\kappa = 1.6754$—asymptotic limit at $h \to \infty$; see Fig. 3.12

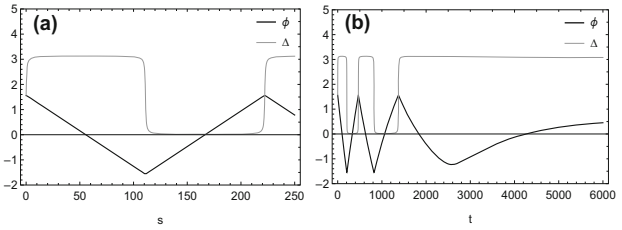

Fig. 3.14 Sample behavior of the phase angles ϕ and Δ at critical fluid height, $h = 0.3666$, and the initial conditions: $P(0) = 0.9999$, $\Delta(0) = \pi/2$, $E(0) = 0.25$: (**a**) variable time scale and (**b**) the original time

more energy of elastic deformations than the inphase mode, and this makes both modes physically different.

Figure 3.14 illustrates the behavior of excitation distribution between the modes in terms of the angle $\phi = \arcsin P$ and the phase shift Δ corresponding to the case (b) of Fig. 3.13. The initial conditions correspond to the rotating mode on the configuration plane $q_1 - q_2$. It is seen that the excitation exchange happens in a nonsmooth way due to the fact that only one of the two NSMs was predominantly

excited at $t = 0$. In this case almost all the energy will drift from one mode to another.

3.3.5 Model of Weakly Coupled Autogenerators

Following [114] consider an ensemble of two linearly coupled generalized van der Pol-Duffing autogenerators that differ from each other by only one coefficient including the so-called frequency detuning parameter σ:

$$\begin{aligned} &\ddot{u}_1 + u_1 + 8\alpha\varepsilon {q_1}^3 + 2\beta\varepsilon(u_1 - u_2) \\ &+ 2\varepsilon(\gamma - 4b{u_1}^2 + 8d{u_1}^4)\dot{u}_1 = 0 \\ &\ddot{u}_2 + (1 + 4\varepsilon\sigma)u_2 + 8\alpha\varepsilon {u_2}^3 + 2\beta\varepsilon(u_2 - u_1) \\ &+ 2\varepsilon(\gamma - 4b{u_2}^2 + 8d{u_2}^4)\dot{u}_2 = 0 \end{aligned} \tag{3.107}$$

In this case, setting $\Omega = 1$ and applying the averaging operator (3.58) to system (3.56) and (3.57) give, respectively,

$$\dot{E} = -2\varepsilon E[\gamma - bE + dE^2 - (b - 3dE)EP^2] \tag{3.108}$$

$$\dot{P} = 2\varepsilon\left[E(b - 2dE)P(1 - P^2) + \beta\sqrt{1 - P^2}\sin\Delta\right] \tag{3.109}$$

$$\dot{\Delta} = 2\varepsilon\left[\sigma - 3\alpha EP - \beta\frac{P}{\sqrt{1 - P^2}}\cos\Delta\right] \tag{3.110}$$

and

$$\dot{\delta} = 1 + \varepsilon\left[3\alpha E(1 + P) + \beta\left(1 - \sqrt{\frac{1 - P}{1 + P}}\cos\Delta\right)\right] \tag{3.111}$$

In the conservative case, when no dissipative terms are present in the original system (3.107), equation of (3.108) takes the form $\dot{E} = 0$, and thus the averaged total energy of both oscillators remains constant during the vibrating process. Otherwise, this energy is varying unless the right-hand side of Eq. (3.108) is zero:

$$\gamma - bE + dE^2 - (b - 3dE)EP^2 = 0 \tag{3.112}$$

It is easy to see the particular case, $E = b/(3d)$ and $\gamma = 2b^2/(9d)$, in which condition (3.112) takes place. Substituting these values of E and γ in (3.109) and (3.110) give the reduced system on the phase plane $\Delta - P$ as

$$\frac{dP}{d\bar{t}} = \frac{b^2}{9\beta d} P(1-P^2) + \sqrt{1-P^2}\sin\Delta$$

$$\frac{d\Delta}{d\bar{t}} = \frac{\sigma}{\beta} - \frac{\alpha b}{\beta d} P - \frac{P}{\sqrt{1-P^2}}\cos\Delta \tag{3.113}$$

where $\bar{t} = 2\varepsilon\beta t$.

The result of numerical integration at the stationary excitation level $E = b/(3d)$ is illustrated in Fig. 3.15. In particular, fragment (a) shows that the temporal mode shapes of phase angles ϕ and Δ tend to stabilize close to the triangle and square waves, respectively. Fragment (b) explains what happens in terms of the excitation distribution index P and the phase shift Δ. As follows from the coherency index Q, which is obtained by the direct integration of the original system, the generators oscillate coherently in the dynamic regime close to the elliptic rotational mode as seen from the fragment (c). During this rotational mode, the excitation is transmitted from one generator to another. The corresponding trajectory in the configuration plane of original variables is shown in fragment (d). Phase transitions happen quickly in a stepwise manner, when only one of the two generators is excited. A fixed phase shift means that oscillators are synchronized. In the case under consideration, the phase shift is practically fixed except for relatively short intervals

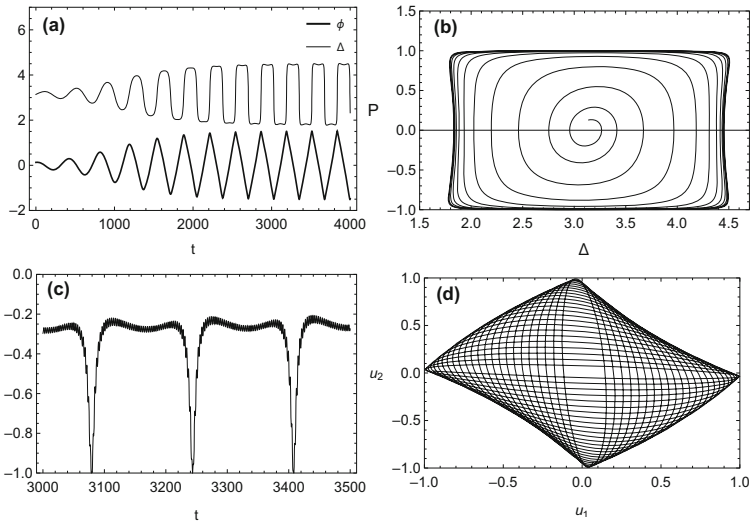

Fig. 3.15 The dynamics of weakly coupled autogenerators in different variables obtained by numerical integration of the original and averaged equations under the stationary total excitation level given by $E(0) = b/(3d)$ and the following values of parameters and initial conditions: $\varepsilon = 0.01$, $\beta = 1.0$, $\alpha = 0.268$, $d = 0.8$, $b = 1.2$, $\sigma = 0$, $\gamma = 2b^2/(9d)$, $\Delta(0) = \pi - 0.001$, $P(0) = 0.128844$

of stepwise switches. Such type of synchronization was noticed and defined as nonconventional synchronization in [135] and then documented in [115].

3.3.6 *Localization of Friction-Induced Vibrations*

The variables$\{E, P, \Delta, \delta\}$ can be used for investigation of different dynamic effects in a coupled set of two coupled oscillators with equal or close to each other natural frequencies regardless of physical meaning of the problem. Following [193], let us consider a chain of n linearly coupled nonlinear oscillators of the mass m driven by friction forces due to the interaction with a continuous stiff surface moving with a constant speed V_b as shown in Figs. 3.16–3.17. The restoring force characteristic of oscillators corresponds to Duffing model, where k_g and k_3 are linear and cubic stiffness coefficients, respectively. In addition to the friction force, each oscillator is subjected to the linear viscous damping with the coefficient of viscosity c. The oscillators are coupled by linear springs of stiffness k. Each mass is under the constant normal load, p. The friction force acting on the jth mass is expressed through its relative velocity as

$$F_j = p\mu(V_b - \dot{q}_j) \tag{3.114}$$

where μ is the so-called friction coefficient, which is usually introduced in a phenomenological way as, for instance [59],

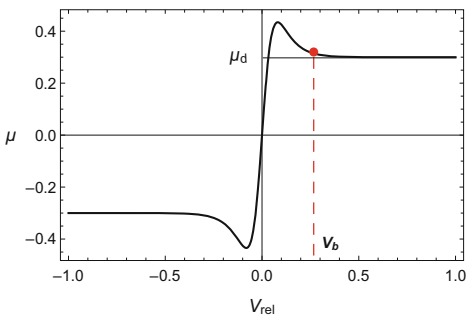

Fig. 3.16 Friction coefficient versus relative velocity (3.115) for the following numerical values: $\alpha_f = \beta_f = 15$, $\mu_\sigma = 0.7$, $\mu_d = 0.3$, and $V_b = 0.23$

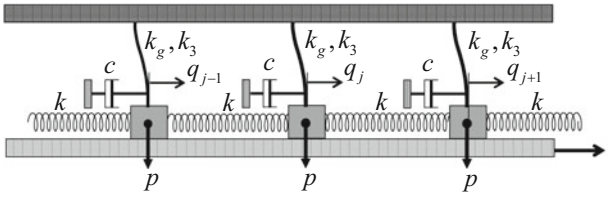

Fig. 3.17 Finite element model of friction interphase

$$\mu(V_{rel}) = \left[\mu_d + \frac{\mu_\sigma - \mu_d}{\cosh(\alpha_f V_{rel})}\right] \tanh(\beta_f V_{rel}) \tag{3.115}$$

Let us introduce the natural frequency of a linearized individual oscillator, $\Omega = \sqrt{k_g/m}$, and scale the parameter of normal load as $\varepsilon = p\Omega/k_g$, assuming that the load is relatively weak. Also, let us introduce two parameters, α and β, characterizing the level of nonlinearity and the strength of coupling, as $k_3/k_g = \varepsilon\alpha$ and $k/k_g = 2\varepsilon\beta$, respectively. The corresponding differential equations of motion are represented in the form

$$\begin{aligned} &\frac{d^2 q_j}{d\bar{t}^2} + q_j + \varepsilon\alpha q_j^3 - 2\varepsilon\beta\left(q_{j-1} - 2q_j + q_{j+1}\right) \\ &\quad = -\varepsilon\left[a\frac{dq_j}{d\bar{t}} + b\left(\frac{dq_j}{d\bar{t}}\right)^3 + d\left(\frac{dq_j}{d\bar{t}}\right)^5\right] \end{aligned} \tag{3.116}$$

where $\bar{t} = \Omega t$ is a natural temporal scale associated with individual linearized oscillators, and a polynomial expansion of the dependence (3.115) was applied to give the following coefficients: $a = \mu'(V_b) + c/p$, $b = \Omega^2\mu^{(3)}(V_b)/6$, and $d = \Omega^4\mu^{(5)}(V_b)/120$.

Below a two mass-spring case is considered by assuming that only one coupling spring is present. As a result, system (3.116) gives the system of two coupled non-conservative oscillators

$$\frac{dq_j}{d\bar{t}} = v_j, \quad \frac{dv_j}{d\bar{t}} = -q_j - f_j; \quad j = 1, 2 \tag{3.117}$$

where

$$\begin{aligned} f_1 &= \varepsilon\alpha q_1^3 + 2\varepsilon\beta(q_1 - q_2) + \varepsilon\left[a\frac{dq_1}{d\bar{t}} + b\left(\frac{dq_1}{d\bar{t}}\right)^3 + d\left(\frac{dq_1}{d\bar{t}}\right)^5\right] \\ f_2 &= \varepsilon\alpha q_2^3 + 2\varepsilon\beta(q_2 - q_1) + \varepsilon\left[a\frac{dq_2}{d\bar{t}} + b\left(\frac{dq_2}{d\bar{t}}\right)^3 + d\left(\frac{dq_2}{d\bar{t}}\right)^5\right] \\ &\quad + 4\varepsilon\sigma q_2 \end{aligned} \tag{3.118}$$

Following Sect. 3.3.2 let us substitute (3.118) in Eqs. (3.56) and (3.57) by setting $\Omega = 1$. Then applying the operator of averaging (3.58) with respect to the fast phase δ gives

$$\begin{aligned} \frac{dE}{d\bar{t}} &= -\frac{1}{8}\varepsilon E\left[8a + 6bE + 5dE^2 + \left(6bE + 15dE^2\right)P^2\right] \\ \frac{dP}{d\bar{t}} &= \frac{1}{4}\varepsilon\left[\left(3bE + 5dE^2\right)P\left(P^2 - 1\right) + 8\beta\sqrt{1 - P^2}\sin\Delta\right] \end{aligned} \tag{3.119}$$

$$\frac{d\Delta}{d\bar{t}} = \frac{1}{4}\varepsilon\left(8\sigma - 3\alpha E P - \frac{8\beta P}{\sqrt{1-P^2}}\cos\Delta\right)$$

$$\frac{d\delta}{d\bar{t}} = 1 + \frac{3}{8}\varepsilon\alpha E(1+P) + \varepsilon\beta\left(1 - \sqrt{\frac{1-P}{1+P}}\cos\Delta\right) \tag{3.120}$$

Analyzing the right-hand side of the first equation in (3.119) reveals the stationary excitation level, $E = E_{stat} = -(2/5)b/d$, which is possible under the condition $d = (1/5)b^2/a$. Taking into account these two relationships brings another two equations of system (3.119) to the form

$$\frac{dP}{ds} = \frac{a}{4\beta}P(1-P^2) + \sqrt{1-P^2}\sin\Delta$$

$$\frac{d\Delta}{ds} = \frac{\sigma}{\beta} + \frac{3a}{4b}\frac{\alpha}{\beta}P - \frac{P}{\sqrt{1-P^2}}\cos\Delta \tag{3.121}$$

where $s = 2\varepsilon\beta\bar{t}$ is a slow time scale associated with the strength of coupling.

System (3.121) represents an autonomous planar case; hence, using phase plane diagrams for its parametric study becomes possible. For instance, analyzing the equilibrium points of system (3.121) versus the cubic nonlinearity, α, shows that the antiphase mode, $(\Delta, P) = (\pi, 0)$ experiences center to saddle bifurcation at $\alpha_* = -4\beta b/(3a)$ by giving rise to the local modes as illustrated in Fig. 3.18.

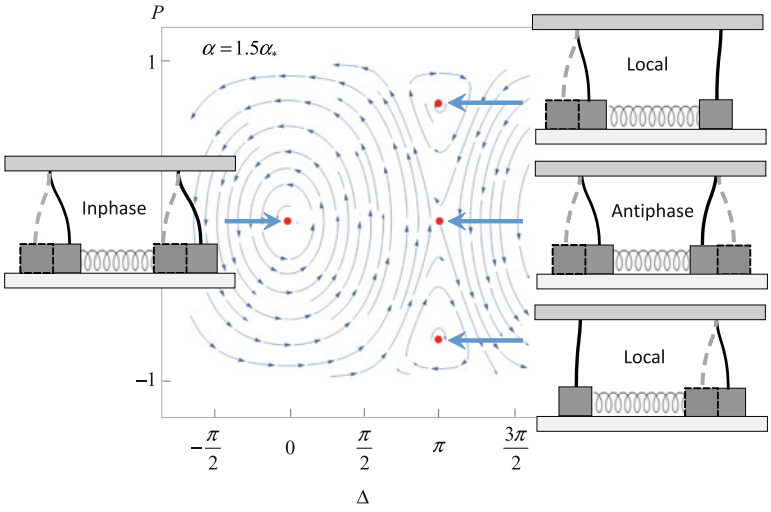

Fig. 3.18 Developed nonlinear mode localization at supercritical nonlinearity according to (3.121) under parameter values [193]: $V_b = 0.23$, $a = 0.1406$, $\beta = 1.0$, $b = -10.43$, $d = 154.72$, and thus $\alpha_* = 98.9015$

3.4 Transition from Normal to Local Modes

The transient mode localization phenomenon is considered below in a mechanical model combined of a simply supported beam with two localized mass attachments enforced by nonlinear springs with hardening characteristics. Two different approaches to the model reduction, such as normal and local mode representations for the beam's center line, are discussed. It is concluded that the local mode discretization brings advantages for the transient localization analysis. Based on the specific coordinate transformations and the idea of averaging, explicit equations describing the energy exchange between the local modes and the corresponding localization conditions are obtained. It was shown that, when the energy is slowly pumped into the system then, at some point, the energy equipartition around the system suddenly breaks and one of the two local modes becomes the dominant energy receiver. The phenomenon is interpreted in terms of the related phase plane diagram. The diagram shows qualitative changes near the image of antiphase mode as the total energy of the system has reached its critical level. A simple closed form expression is obtained for the corresponding critical time estimate. The material below is an update of reference [189].

3.4.1 Model Description

The model under investigation represents a simply supported elastic beam of length l with two masses attached to the beam and connected to the base by nonlinear springs as shown in Fig. 3.19. The corresponding differential equation of motion and boundary conditions are, respectively,

$$\rho A \frac{\partial^2 w}{\partial t^2} + EI \frac{\partial^4 w}{\partial y^4} = f_1(t)\delta(y - y_1) + f_2(t)\delta(y - y_2) \tag{3.122}$$

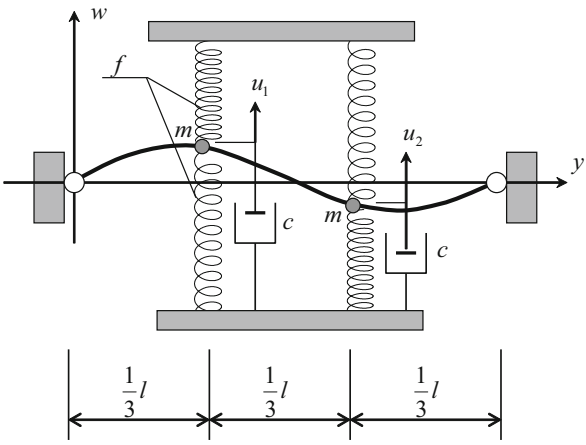

Fig. 3.19 The mechanical model admitting both normal and local mode motions; all the springs have hardening restoring force characteristics

and

$$w(t, y)|_{y=0,l} = 0, \quad \frac{\partial^2 w(t, y)}{\partial y^2}|_{y=0,l} = 0 \tag{3.123}$$

where

$$f_i(t) = -f[w(t, y_i)] - c\frac{\partial w(t, y_i)}{\partial t} - m\frac{\partial^2 w(t, y_i)}{\partial t^2}; \quad i = 1, 2 \tag{3.124}$$

are transverse forces applied to the beam from masses attached at the points $y = y_{1,2}$.

It will be assumed that the structure is symmetric with respect to the middle of the beam, $y = l/2$, such that

$$y_1 = l/3 \quad \text{and} \quad y_2 = 2l/3 \tag{3.125}$$

Below we consider the case of the hardening restoring force characteristics of the springs and show that, under appropriate conditions, a slow energy inflow leads to the localization of vibration modes. As a result, the system energy is spontaneously shifted to either the left or the right side of the beam due to the so-called symmetry breaking effect. The adiabatic (slow) energy increase means that the energy source has a minor or no direct effect on the mode shapes. For simulation purposes, such energy inflow is provided by the assumption that the viscous damping coefficient c is sufficiently small and negative; the physical basis for such an assumption was discussed in [187, 188]. This remark, which is substantiated below by the corresponding numerical values of the parameters, is important to follow; otherwise, the phenomenon, which is the focus of this paper, may not be developed. In contrast, the dissipation ($c > 0$) can lead to a spontaneous dynamic transition from local to normal modes, when the total energy reaches its sub-critical level.

Recall that the presence of Dirac δ-functions in Eq. (3.122) requires a generalized interpretation of the differential equation of motion in terms of distributions [208]. The corresponding compliance is provided by further model reduction based on the Bubnov-Galerkin approach, which actually switches from the point-wise to the integral interpretation of equations.

3.4.2 Normal and Local Mode Coordinates

Normal Mode Coordinates

Let us evaluate two possible ways to discretizing the model (3.122). The minimum number of modes (two) will be maintained to capture the effect of interest. The conventional normal mode representation for the boundary value problem (3.122)–(3.123) is

$$w(t, y) = w_1(t) \sin \frac{\pi y}{l} + w_2(t) \sin \frac{2\pi y}{l} \tag{3.126}$$

Substituting (3.126) in (3.122) and applying the standard Bubnov-Galerkin procedure give

$$\ddot{w}_1 + \frac{3}{3m + Al\rho} \left(c\dot{w}_1 + \frac{\pi^4 EI}{3l^3} w_1 \right) + F_1(w_1, w_2) = 0 \tag{3.127}$$
$$\ddot{w}_2 + \frac{3}{3m + Al\rho} \left(c\dot{w}_2 + 16\frac{\pi^4 EI}{3l^3} w_2 \right) + F_2(w_1, w_2) = 0$$

where $F_i(w_1, w_2) = F(w_1 + w_2) + (-1)^{i+1} F(w_1 - w_2)$, and

$$F(z) = \frac{\sqrt{3}}{3m + Al\rho} f\left(\frac{\sqrt{3}}{2} z \right) \tag{3.128}$$

Equations (3.127) are decoupled in the linear terms related to the elastic beam center line, whereas the modal coupling is due to the spring nonlinearities participating in $F(z)$.

Local Mode Coordinates

Alternatively, the model can be discretized by introducing the local mode coordinates determined by the spring locations

$$u_i(t) = w(t, y_i); \quad i = 1, 2 \tag{3.129}$$

Substituting (3.125) in (3.126) and taking into account (3.129) reveal simple links between the normal and local coordinates as

$$u_1 = \frac{\sqrt{3}}{2}(w_1 + w_2), \quad u_2 = \frac{\sqrt{3}}{2}(w_1 - w_2) \tag{3.130}$$

or, inversely,

$$w_1 = \frac{\sqrt{3}}{3}(u_1 + u_2), \quad w_2 = \frac{\sqrt{3}}{3}(u_1 - u_2) \tag{3.131}$$

Substituting (3.131) in (3.126) gives the local mode representation for the beam center line

$$w(t, y) = u_1(t)\psi_1 \left(\frac{\pi y}{l} \right) + u_2(t)\psi_2 \left(\frac{\pi y}{l} \right) \tag{3.132}$$

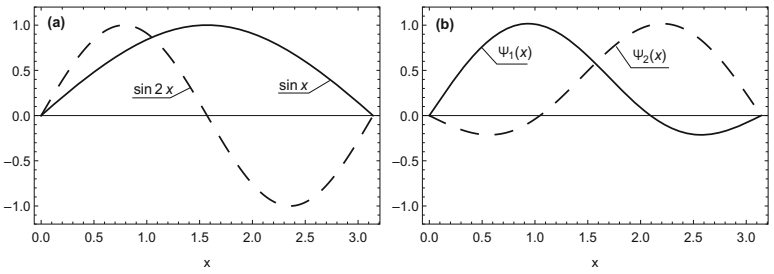

Fig. 3.20 Two types of spatial basis for simply supported beams: (**a**) normal modes and (**b**) local mode shape functions

where the local mode shape functions are defined as

$$\begin{bmatrix} \psi_1(x) \\ \psi_2(x) \end{bmatrix} = \frac{\sqrt{3}}{3} \begin{bmatrix} 1 & 1 \\ 1 & -1 \end{bmatrix} \begin{bmatrix} \sin x \\ \sin 2x \end{bmatrix} \tag{3.133}$$

Both normal and local mode shape functions are shown in Fig. 3.20a and b, respectively. Transformation (3.133) can be generalized for a greater number of modes. Note that functions (3.133) satisfy the following orthogonality condition

$$\int_0^{\pi} \psi_i(x)\, \psi_j(x)\, dx = \frac{\pi}{3}\delta_{ij} \tag{3.134}$$

where δ_{ij} is the Kronecker symbol.

The differential equations for the local mode amplitudes, $u_1(t)$ and $u_2(t)$, can be derived by substituting (3.132) in the partial differential equation (3.122) and then applying Bubnov-Galerkin procedure with orthogonality condition (3.134). Alternatively the equations can be obtained by substituting (3.131) in (3.127) and conducting straightforward algebraic manipulations. Finally the local mode equations take the form

$$\ddot{u}_1 + \frac{3}{3m + Al\rho}\left[c\dot{u}_1 + \frac{\pi^4 EI}{6l^3}(17u_1 - 15u_2) + f(u_1)\right] = 0 \tag{3.135}$$

$$\ddot{u}_2 + \frac{3}{3m + Al\rho}\left[c\dot{u}_2 + \frac{\pi^4 EI}{6l^3}(17u_2 - 15u_1) + f(u_2)\right] = 0$$

Further consider Duffing's type polynomial approximation for the springs restoring force characteristic, $f(z) = kz + az^3$.

Symmetry Breaking with Energy Localization

Let us represent equations (3.135) as a set of four first-order equations for the system state variables

$$\begin{aligned} \dot{u}_1 &= v_1 \\ \dot{u}_2 &= v_2 \\ \dot{v}_1 &= -\Omega^2 u_1 - f_1 \\ \dot{v}_2 &= -\Omega^2 u_2 - f_2 \end{aligned} \tag{3.136}$$

where

$$\begin{aligned} f_1 &= \varepsilon(-\Omega^2 u_2 + \zeta v_1 + \alpha u_1^3) \\ f_2 &= \varepsilon(-\Omega^2 u_1 + \zeta v_2 + \alpha u_2^3) \end{aligned} \tag{3.137}$$

and the following set of parameters and assumptions are introduced:

$$\Omega = \sqrt{\frac{6kl^3 + 17\pi^4 EI}{2l^3(3m + Al\rho)}} = O(1), \quad \varepsilon = \frac{15\pi^4 EI}{6kl^3 + 17\pi^4 EI} << 1 \tag{3.138}$$

$$\zeta = \frac{3c}{(3m + Al\rho)\varepsilon} = O(1), \quad \alpha = \frac{3a}{(3m + Al\rho)\varepsilon} = O(1)$$

From the physical standpoint, relationships (3.138) mean that the beam is flexible enough compared to the linear stiffness of springs, whereas both the viscosity effect and nonlinearity are relatively weak as compared to the beam bending rigidity. Note that localized spring forces may practically trigger high modes of the flexible beam and thus invalidate the two modes' approximation represented by relationship (3.126). Nonetheless, in the current illustrating model, a role of the beam is secondary. As follows from system (3.136), the beam just provides a weak coupling between the oscillators. Therefore a more detailed modeling could incorporate the high modes as a perturbation to the coupling effect.

Following Sect. 3.3.1, substituting (3.137) in (3.56) and (3.57), and conducting the averaging give

$$\begin{aligned} \dot{E} &= -\varepsilon\zeta E \\ \dot{P} &= \varepsilon\Omega\sqrt{1 - P^2}\sin\Delta \\ \dot{\Delta} &= -\varepsilon\Omega\left(\frac{3\alpha}{4\Omega^4}E + \frac{\cos\Delta}{\sqrt{1 - P^2}}\right)P \end{aligned} \tag{3.139}$$

and

$$\dot{\delta} = \Omega + \frac{3\varepsilon\alpha}{8\Omega^3}E(1+P) - \frac{1}{2}\varepsilon\Omega\sqrt{\frac{1-P}{1+P}}\cos\Delta \tag{3.140}$$

If the viscosity is negative,[5] $\zeta < 0$, then Eqs. (3.139) describe transition to the local mode as the system energy increases; see Fig. 3.21 for illustration. The energy partitioning parameter P is varying within the interval $-1 \le P \le 1$. The ends of the interval obviously correspond to the local modes, whereas its center $P = 0$ corresponds to the normal modes: $\Delta = 0$-inphase, and $\Delta = \pi$-antiphase; recall transformation (3.44). Linearizing system (3.139) in the vicinity of stationary points $(\Delta, P) = (0, 0)$ and $(\Delta, P) = (\pi, 0)$, assuming the variable E is "frozen," and eliminating the phase variable give

$$\ddot{P} + \varepsilon^2\Omega^2\left(1 \pm \frac{3\alpha}{4\Omega^4}E\right)P = 0 \tag{3.141}$$

where plus or minus sign in the parenthesis corresponds to the inphase or antiphase mode, respectively.

It follows from the form of Eq. (3.141) that a localized mode can branch out of the antiphase mode, when $E = E^* = 4\Omega^4/(3\alpha)$. In the case of negative viscosity, the first equation in (3.139) gives $E = E_0\exp(\varepsilon|\zeta|t)$. Therefore, the critical system excitation level E^* will be reached regardless of the initial number E_0, when $t = t^*$:

$$t^* = \frac{1}{\varepsilon|\zeta|}\ln\frac{4\Omega^4}{3\alpha E_0} \tag{3.142}$$

The data of Fig. 3.21 gives $E_0 = 1.36585 \times 10^{-5}$, $E^* = 1.42116 \times 10^{-2}$, and expression (3.142) generates the number $t^* = 3580.42$, in a reasonable agreement with Fig. 3.21.

3.5 Autolocalized Modes in Nonlinear Coupled Oscillators

Below, the term *autolocalized* means that the system itself may come into the nonlinear local mode regime and stay there regardless of initial energy distribution among its particles. As follows from Poincaré recurrence theorem, such phenomena are rather impossible within the class of conservative systems [16]. Nonetheless, interactions between the system particles can be designed in specific ways in order to achieve desired phenomena. It is assumed that such a design can be implemented practically by using specific electric circuits and possibly mechanical actuators. On macro-levels, the autolocalization may help to optimize vibration suppression.

[5] Possible physical mechanisms of the negative viscosity are not discussed here since the negative damping is used only for simulation of a slow energy inflow into the system.

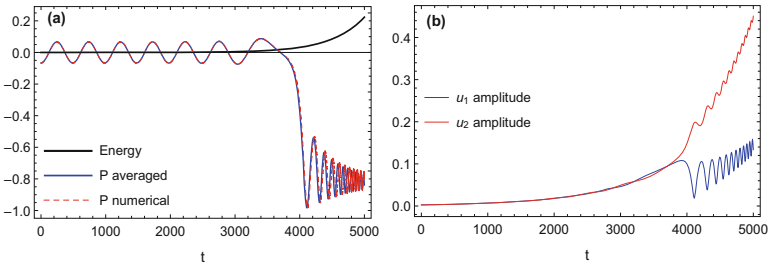

Fig. 3.21 Symmetry breaking followed by sudden transition from normal to local mode vibration as the system energy has reached its critical value: (**a**) energy distribution and (**b**) local mode amplitudes; the following parameters were taken for numerical simulations: $\varepsilon = 0.009$, $\zeta = -0.2156$, $\Omega = 1.4217$, $\alpha = 383.29$, and the initial normal mode amplitudes at zero velocities are $w_1(0) = 0.0001$ and $w_2(0) = -0.003$

Some results from the previous publication [179] are reproduced below after some notation modifications for a better coherency with the current text. Let us consider an array of N harmonic oscillators, such that each of the oscillators interacts with only the nearest neighbors. The corresponding differential equations of motion are of the form

$$\ddot{x}_j + \Omega^2 x_j = \beta(x_{j-1} - 2x_j + x_{j+1}) +$$

$$+ \alpha[(E_j - E_{j-1})E_{j-1} - (E_{j+1} - E_j)E_{j+1}]\dot{x}_j \tag{3.143}$$

$$E_j = \frac{1}{2}(\dot{x}_j^2 + \Omega^2 x_j^2); \qquad j = 1, ..., N \tag{3.144}$$

where $E_j = E_j(t)$ is the total energy[6] of the jth oscillator under the boundary conditions of fixed ends, $E_0(t) \equiv E_{N+1}(t) \equiv 0$; and Ω, β, and α are constant parameters of the model.

On the right-hand side of Eq. (3.143), two groups of terms describe the coupling between the oscillators. If $\alpha = 0$ then the only linear coupling remains. In this case, under special initial conditions, N different coherent periodic motions, i.e., linear normal modes, can exist. Any other motion is combined of the linear normal mode motions, whereas the energy is conserved on each of the modes the way it was initially distributed between the modes. In other words, no energy localization is possible on individual particles if $\alpha = 0$.

Another group of terms, including the common factor α, has the opposite to the linear elastic interaction effect. These nonlinear terms are to simulate a

[6] Note that the concept of energy for individual oscillators becomes somewhat ambiguous in the presence of coupling and nonconservative terms. Hence expression (3.144) should rather be viewed as Lyapunov function.

possible competition between the oscillators leading to a one-way energy flow to the neighbor whose energy is greater. Such kind of interaction dominates when the total system energy is large enough to involve high degrees of the coordinates and velocities.

Let us introduce the complex conjugate variables $\{A_j(t), \bar{A}_j(t)\}$ into Eqs. (3.143) according to relationships

$$x_j = \frac{1}{2}[A_j \exp(i\Omega t) + \bar{A}_j \exp(-i\Omega t)]$$
$$\dot{x}_j = \frac{1}{2} i\Omega [A_j \exp(i\Omega t) - \bar{A}_j \exp(-i\Omega t)] \tag{3.145}$$

where the following compatibility condition is imposed

$$\frac{dA_j}{dt} \exp(i\Omega t) + \frac{d\bar{A}_j}{dt} \exp(-i\Omega t) \tag{3.146}$$

In terms of the complex amplitudes, the total energy of individual oscillator (3.144) takes the form

$$E_j = \frac{1}{2}\Omega^2 A_j \bar{A}_j = \frac{1}{2}\Omega^2 |A_j|^2 \tag{3.147}$$

When $\beta = \alpha = 0$, the system is decomposed into N uncoupled oscillators leading to a constant solution in the new variables. In general case, substituting (3.145) in (3.143), taking into account (3.146), and applying the averaging with respect to the phase $z = \Omega t$, give the set of equations

$$\dot{A}_j = -\frac{i\beta}{2\Omega}(A_{j-1} - 2A_j + A_{j+1}) +$$
$$+ \frac{\alpha\Omega^4}{8}\left[\left(|A_j|^2 - |A_{j-1}|^2\right)|A_{j-1}|^2 - \left(|A_{j+1}|^2 - |A_j|^2\right)|A_{j+1}|^2\right] A_j \tag{3.148}$$
$$(j = 1, ..., N)$$

where the conjugate equations are omitted.

Let us consider first the case of two coupled oscillators ($N = 2$), when system (3.148) is reduced to

$$\dot{A}_1 = -\frac{i\beta}{2\Omega}(A_2 - 2A_1) + \frac{\alpha\Omega^4}{8}\left(|A_1|^2 - |A_2|^2\right)|A_2|^2 A_1 \tag{3.149}$$
$$\dot{A}_2 = -\frac{i\beta}{2\Omega}(A_1 - 2A_2) + \frac{\alpha\Omega^4}{8}\left(|A_2|^2 - |A_1|^2\right)|A_1|^2 A_2$$

This system has the integral

$$K = |A_1|^2 + |A_2|^2 = 2(E_1 + E_2)/\Omega^2 = const.$$

As a result, the dimension of phase space is reduced by introducing the phases $\varphi_1(t)$, $\varphi_2(t)$ and $\psi(t)$ as

$$A_1 = \sqrt{K}\cos\psi\exp(i\varphi_1), \qquad A_2 = \sqrt{K}\sin\psi\exp(i\varphi_2) \tag{3.150}$$

where ψ determines the energy distribution between the oscillators as

$$\tan\psi = \frac{|A_2|}{|A_1|} = \sqrt{\frac{E_2}{E_1}} \qquad (0 \le \psi < \pi/2) \tag{3.151}$$

Substituting (3.150) in system (3.149) and then considering separately its real and imaginary parts give

$$\begin{aligned}
\dot{\varphi}_1 &= \frac{\beta}{\Omega} - \frac{\beta}{2\Omega}\tan\psi\cos(\varphi_2 - \varphi_1) \\
\dot{\varphi}_2 &= \frac{\beta}{\Omega} - \frac{\beta}{2\Omega}\cot\psi\cos(\varphi_2 - \varphi_1) \\
\dot{\psi} &= -\frac{\beta}{2\Omega}\sin(\varphi_2 - \varphi_1) - \frac{1}{32}\alpha K^2\Omega^4\sin 4\psi
\end{aligned} \tag{3.152}$$

Introducing the phase shift $\Delta = \varphi_2 - \varphi_1$ and new temporal variable $p = \Omega t/\beta$ give

$$\begin{aligned}
\frac{d\Delta}{dp} &= -\cot 2\psi\cos\Delta \\
\frac{d\psi}{dp} &= -\frac{1}{2}(\sin\Delta + \lambda\sin 4\psi)
\end{aligned} \tag{3.153}$$

where λ is a dimensionless parameter related to the total energy of both oscillators as

$$\lambda = \frac{\alpha K^2\Omega^5}{16\beta} = \frac{\Omega\alpha}{4\beta}(E_1 + E_2)^2 \tag{3.154}$$

System (3.153) is periodic with respect to both phases, Δ and ψ. As a result, its phase plane has the periodic cell-wise structure. Let us consider just one cell,

$$R_0 = \left\{-\frac{\pi}{2} < \Delta < \frac{\pi}{2}, 0 < \Psi < \frac{\pi}{2}\right\} \tag{3.155}$$

including the stationary point

$$(\Delta, \psi) = (0, \pi/4) \tag{3.156}$$

As follows from (3.150) and (3.151), point (3.156) represents the inphase vibration with $E_1 = E_2$. Linearizing system (3.153) near this stationary and then solving the corresponding characteristic equation give the following couple of roots:

$$r_{1,2} = \lambda \pm i\sqrt{1-\lambda^2} \tag{3.157}$$

Expression (3.157) determines the low excitation interval $0 < \lambda < 1$ of a qualitatively similar system behavior. Point (3.156) is unstable by Lyapunov for positive λ, while no other stationary points exist within the rectangular cell (3.155). As a result, the system trajectory is eventually attracted to the boundary of rectangular R_0 (3.155) as shown in Fig. 3.22a and b. This is a periodic limit cycle whose period is found in a closed form,

$$T = 2\int_0^{\pi/2} \frac{d\psi}{1-\lambda\sin 4\psi} - 2\int_{\pi/2}^{0} \frac{d\psi}{1+\lambda\sin 4\psi} = \frac{2\pi}{\sqrt{1-\lambda^2}} \tag{3.158}$$

where the horizontal pieces of the boundary ∂R_0 have zero contribution as those passed momentarily by the system (3.153). This is confirmed also by the diagrams in Fig. 3.23a, c and b, d showing stepwise jumps of the variable $\Delta(p)$ in steady-state limits.

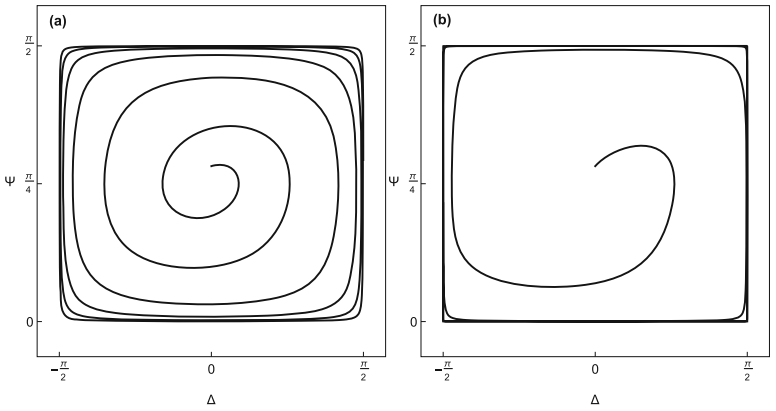

Fig. 3.22 (**a**) Low-energy transition to the nonsmooth limit cycle; numerical solution obtained for the following system parameter and initial conditions: $\lambda = 0.2$; $\Delta(0) = 0.0$, $\Psi(0) = \pi/4 + 0.1$. (**b**) Transition to the nonsmooth limit cycle under the energy level approaching its critical value; the numerical solution obtained for the following system parameter and initial conditions: $\lambda = 0.6$; $\Delta(0) = 0.0$, $\Psi(0) = \pi/4 + 0.1$

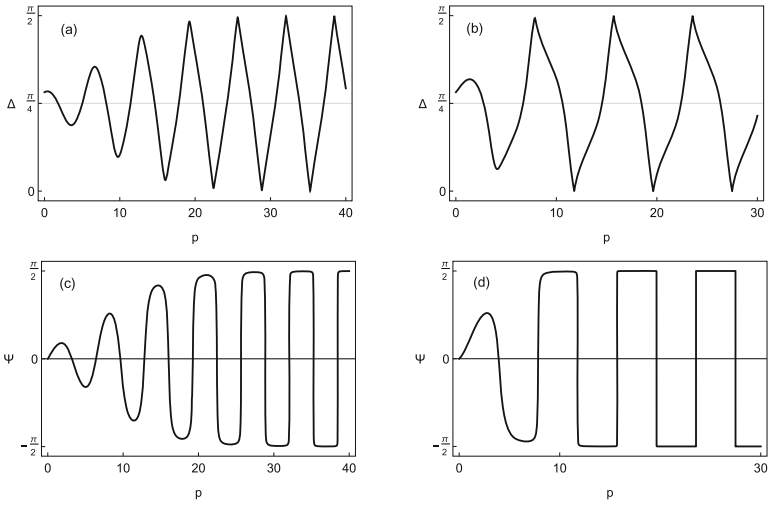

Fig. 3.23 (**a**) and (**c**): Low-energy transition to the "impact" limit cycle of phase variables at $\lambda = 0.2$; (**b**) and (**d**) Transition to the "impact" limit cycle of phase variables at $\lambda = 0.6$

Expression (3.158) shows that $T \to \infty$ as $\lambda \to 1$. The infinity long period means that there is only one-way energy flow in the system. As a result, the energy is eventually localized on one of the oscillators. The corresponding total critical energy value is determined by substituting $\lambda = 1$ in (3.154). This gives

$$E_1 + E_2 = 2\sqrt{\frac{\beta}{\Omega\alpha}} = E^* \tag{3.159}$$

If $E_1 + E_2 < E^*$ then periodic energy exchange with the period $T = \beta P/\Omega$ takes place, but no localization is possible. Therefore, in order to be localized on one of the oscillators, the total system energy must be large enough. Note that the transition to localized mode of this model happens through nonsmooth limit cycle along which the dynamics of phase variables, Ψ and Δ, resembles the behavior of coordinate and velocity of impact oscillator;[7] see Fig. 3.23. It was found later that such types of trajectories represent quite a general situation that may occur in the dynamics of interacting oscillators in terms of the specific phase coordinates. As a result the concept of limiting phase trajectories (LPT) was introduced in [133] as complementary nonstationary alternative to (stationary) normal mode motions.

[7] As already mentioned, the possibility of "vibro-impact dynamics" of phase variables was noticed later in [133] when considering another model of nonlinear beats.